ACS APPLIED POLYMER MATERIALS

pubs.acs.org/acsapm

Article

Comparative Mechanochromic Performance of Perylene Diimide-Doped Polyurethanes: Blending vs Bonding

Emma Contini, Valentina Antonia Dini, Andrea Rozzi, Damiano Genovese, Nelsi Zaccheroni, Alessandro Pedrini, Enrico Dalcanale, Roberta Pinalli, and Chiara Gualandi*

Cite This: ACS Appl. Polym. Mater. 2024, 6, 669−680

Read Online

ACCESS | Metrics & More | Article Recommendations | Supporting Information

ABSTRACT: The research on mechanochromic polymers encompasses the use of aggregachromic dyes loaded into various polymeric matrices. However, in recent years, the covalent incorporation of these dyes into polymeric chains has gained momentum in the direction of boosting the sensitivity in mechanochromic materials. This work compares the mechanochromism of a thermoplastic polyurethane containing a perylene diimide probe, either bonded to an "ad hoc" synthesized polyurethane or simply blended. The goal was to determine how the dye concentration and the two incorporation approaches affect the mechanochromic performance. The results show that bonding the chromophore to the polymeric chains lowers its tendency to aggregate, thus leading to a less perceivable color change than that of dispersed dye systems under uniaxial tensile deformation. Conversely, loading−unloading cycles and stress relaxation experiments provide evidence that the covalent incorporation of the dye provides a higher sensitivity with an improved correspondence between the mechanical and optical behavior.

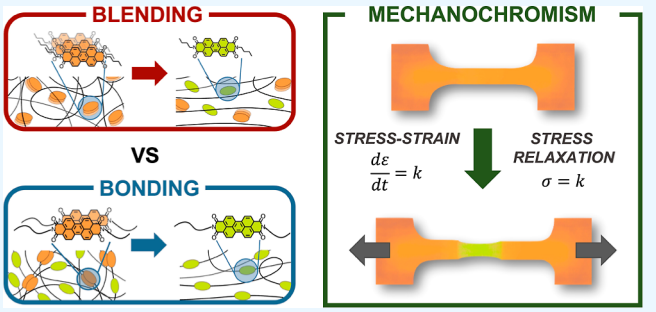

KEYWORDS: *perylene diimide, polyurethane, aggregachromic dye, stimuli-responsive materials, mechanochromic materials*

1. INTRODUCTION

Detecting the occurrence of force-induced bond breakage in polymeric materials is crucial for understanding the mechanisms of failure and preventing material malfunction.[1,2] A broad spectrum of mechanochromic polymers has been proposed to accomplish this task.[3] They belong to the class of stimuli-responsive materials as their optical properties vary in response to a mechanical stimulus.[4]

Two major strategies can be used to develop this type of material: the synthesis of intrinsically mechanochromic polymers and the addition of a mechanochromic additive to a polymeric matrix.[3−6] Intrinsically mechanochromic polymers are obtained by covalently linked chromophoric units (often called "mechanophores") to the macromolecular chains.[7] These chromophores are characterized by mechanically cleavable bonds (or interactions), which are broken when a specific limit force is exceeded, thus providing the desired stimuli responsiveness.[8] Several mechanophores exhibiting modifications in the optical properties upon covalent bond scission have been reported in the literature. For example, spiropyrans,[8−12] 1,2-dioxetanes,[13−15] diarylbibenzofuranones,[16−18] rhodamines,[19,20] naphthopyrans,[21] and oxazines[22] have been extensively employed for stress sensing in polymers. However, since the primary working principle of these motifs is covalent bond rupture, their ability to sense stresses in the low-strain regime of polymer deformation is often limited. Additionally, their applications are restricted because the mechanical activation of such mechanophores is usually not immediately reversible without the use of an external stimulus.[23] Polymers containing dyes whose mechanochromic response is based on noncovalent interactions have the potential to overcome these significant limitations. The development of this last strategy favors the industrial acceptance of mechanochromic probes based on cost-and-benefit analysis, especially in terms of preparation steps and times.[24]

Current research on this topic mainly focuses on using aggregachromic dyes, namely, pyrene derivatives,[23] oligo(*p*-phenylenevinylene),[25,26] and perylene.[27−29] These dyes are characterized by absorption and emission properties that are susceptible to the intermolecular distance and relative orientation of the chromophore molecules with respect to each other, making them highly sensitive to ratiometric signaling units. Typically, aggregated dye molecules present a red-shifted emission in the pristine material compared with the

Received: September 25, 2023
Revised: November 14, 2023
Accepted: November 17, 2023
Published: December 8, 2023

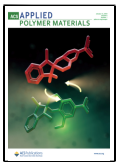

isolated dye. Conversely, when a mechanical stimulus induces disaggregation, the emission is blue-shifted (monomer-dominated emission). The presence of two distinct emission bands makes this type of dye extremely interesting for real-life applications since the ratio between the emission intensity at λ_{em}^{max} (monomer) and the emission intensity at λ_{em}^{max} (aggregate) can be used to monitor the disaggregation process. Furthermore, if a mathematical correlation exists between the ratiometric intensity and the deformation applied, then the material will behave as an intrinsic strain sensor.

The properties of these dyes make them suitable to produce both covalently functionalized mechanochromic polymers and mechanochromic blends containing the dye as a dispersed additive.[30−36]

The latter approach has also attracted significant interest thanks to its high versatility, which allows obtaining many different mechanochromic polymers in a simple and fast way. However, especially with large-sized aggregates and in materials with high segmental mobility, the lack of strong interactions between the polymeric matrix and the dye molecules can lead to poor disaggregation and, thus, to a limited mechanochromic response.[7]

These issues are behind the current interest in developing covalently functionalized systems bearing aggregachromic mechanophores. For example, Weder and co-workers reported cyano-OPV (oligo(*p*-phenylenevinylene)) dyes[25,26,31] and perylene diimide derivatives[27,28] bound to the main polymeric chains, while, more recently, Pucci and co-workers developed a pyrene-grafted styrene-*b*-(ethylene-*co*-butylene)-*b*-styrene polymer.[23] Until now, a limited number of works present a thorough comparison between the blended and the corresponding covalently functionalized systems.[23,27,31] In these cases, the latter always provided a better mechanochromic response than its dispersed analogous. This result is attributed to the different disaggregation mechanisms that occur in covalently functionalized and blended systems. More specifically, it is hypothesized that disaggregation through conformational change, occurring in the bonded systems, is more efficient than the shear-induced one, occurring in the blended systems.[26] These findings were achieved thanks to smart molecular design. Weder and co-workers synthesized mechanochromic polymers in which the dyes were cleverly linked to the chain by fixing the distance between the chromophore.[27] Differently, Pucci and co-workers spatially confined the dye through phase separation.[23] By exploiting these kinds of molecular designs, it was possible to overcome the reduced tendency to aggregation of covalently bound dyes and to obtain the aggregation degree required to achieve a relevant mechanochromic response. In this context, it becomes interesting to better understand the outcomes of the two approaches (bonding vs blending) by expanding the comparison to simpler polymer systems.

In this study, blended and covalently bound systems were compared by using perylene derivatives (**Per**) in a commercial thermoplastic polyurethane (**TPU**). The covalently bound system was realized by mixing **TPU** with a second PU (named **PolyPer**), bearing **Per** in the main chain. The blended system was attained by blending the **TPU** with the free chromophore and adding, at the same time, a second PU (named **Poly**) not containing the dye. Therefore, these two systems differed only in the dye incorporation approach, keeping constant the chemical structure and the composition of the polymer matrix (**TPU-Poly**). Differently from previous reports,[27,28] **PolyPer** bearing the dye in the main chain was synthesized without controlling the chromophore distribution along the chain, aiming for a straightforward and potentially scalable synthetic procedure. Different concentrations of both bonded and blended chromophores were tested. The photophysical properties of the films were measured at rest and under tensile deformation in stress−strain tests and stress relaxation experiments.

2. EXPERIMENTAL SECTION

2.1. Materials and Methods. All used solvents were of reagent quality and were commercially purchased. All solvents were dried and distilled by using standard procedures. All of the purchased starting materials were used without further purification.

NMR spectra were recorded on a Bruker AVANCE 400 (400 MHz) and a JEOL ECZ600R (600 MHz) spectrometer at 298 K. All chemical shifts (δ) were reported in ppm relative to the proton resonances resulting from incomplete deuteration of the NMR solvents.

High-resolution MALDI-TOF was performed on an AB SCIEX MALDI TOF−TOF 4800 Plus instrument (matrix: a-cyano-4-hydroxycinnamic acid). High-resolution electrospray ionization mass spectrometry (HR-ESI-MS) was performed on a mass spectrometer LTQ ORBITRAP XL Thermo.

GPC was carried out using a KNAUER system equipped with a refractive index detector and a TSKgel SuperHM-M column (length = 150 mm and internal diameter = 6 mm). Tetrahydrofuran (THF) was used as an eluant with a 0.6 mL min^{-1} flow and sample concentrations of about 5 mg mL^{-1}. The analyzed samples were solubilized in THF, stirred overnight, and filtered on a 0.450 μm PTFE filter. A molecular weight calibration curve was obtained with polystyrene standards in the molecular weight range 580−990,500 g mol^{-1}.

UV−vis absorption spectroscopy was performed using a Cary 5000 UV−vis−NIR spectrophotometer (Agilent).

The emission spectra were recorded with an Edinburgh FLS920 fluorometer equipped with a high-speed HS773-04 photomultiplier, Hamamatsu R928P.

Emission spectra in the solid state were acquired by exploiting a Thorlabs compact spectrometer (CCS200M, optical fiber with a 200 μm apical aperture) coupled to a 365 nm LED (ThorLabs SOLIS-365c) as the near-field probe.

Differential scanning calorimetry (DSC) was carried out using a Q2000 DSC apparatus (TA Instruments) equipped with a refrigerated cooling system (RCS90). The analyses were performed on 4−6 mg samples placed inside aluminum pans under a nitrogen flow. The samples under analysis were subjected to three heating scans at a rate of 20 °C min^{-1} alternated with two cooling scans, the first of which was a fast cooling (quenching) and the second of which was a controlled cooling scan at 10 °C min^{-1}.

Dynamic mechanical thermal analysis (DMTA) was carried out on films (gauge length = 10 mm, width = 5 mm, and thickness = 0.2−0.5 mm) by means of a TA Instrument dynamic mechanical analyzer (DMA Q800) under a tensile configuration. The specimens were tested with a heating ramp from −140 to 200 °C at 3 °C·min^{-1}, adopting a frequency of 1 Hz under displacement control.

Stress−strain tests were conducted using an Instron Testing Machine 4465 and the Series IX software package. Dog-bone-shaped samples were prepared following ASTM D1708[37] (gauge length = 14 mm, width = 5 mm, and thickness = 0.2−0.5 mm) and were tested in the traction mode with a load cell of 100 N. The crosshead speed was set at 200 mm·min^{-1}. Cyclic deformation tests were carried out with the same setup on dog-bone samples. Samples were stretched using a crosshead speed of 200 mm·min^{-1} up to 200% of deformation, and the deformation was then relaxed to 100% using a crosshead speed of 5 mm·min^{-1}. This cycle was repeated four times.

Stress relaxation tests were carried out with the same setup on dog-bone samples. Samples were stretched using a crosshead speed of 200 mm·min^{-1} up to 300% of deformation, which was kept constant for 30 min.

https://doi.org/10.1021/acsapm.3c02284
ACS Appl. Polym. Mater. 2024, 6, 669−680

During stress−strain, stress relaxation, and cyclic tests, emission spectra were acquired by exploiting a Thorlabs compact spectrometer (CCS200M, optical fiber with a 200 μm apical aperture) coupled to a 365 nm LED (ThorLabs SOLIS-365c) as the near-field probe. Spectra were recorded at a 10 Hz frequency in stress−strain analysis, while, in stress relaxation analysis, a 1 Hz frequency was employed for the first 60 s of the experiment, and a 0.03 Hz frequency was employed for the remaining time of the experiment. In cyclic tests, spectra were recorded with a 2 Hz frequency.

2.2. Synthesis. *2.2.1. N,N′-Bis(4-Amino-1-butyl)perylene-3,4,9,10-tetracarboxylic Acid Bisimide (Per).* In a pressure-tight microwave tube under nitrogen (CEM Discover purchased from CEM Corp, 3 mm thick, 10 mL volume), 100 mg of perylene-3,4,9,10-tetracarboxylic bisanhydride were suspended in 5 mL of dry *N*,*N*-dimethylformamide (DMF), and 2 equiv of butyl amine were added. The red suspension was sonicated for 5 min before heating under microwave irradiation at 50 W for 10 min. The heating was repeated for five cycles, with cooling intervals of 5 min. The maximum temperature was set at 200 °C. After the solution was cooled, the solution turned dark red. The reaction was quenched by adding 50 mL of NaOH 1 M and then stirred for 30 min (Scheme S1). The obtained precipitate was filtered, washed abundantly with water until neutral pH, and finally dried using a vacuum pump. The final product was obtained as a brown-red solid. Yield 49%.

^{1}H NMR (CF_3COOD, 600 MHz, 298 K): δ (ppm) 8.89−8.85 (m, 8H, HA and HB), 4.38 (bt, 4H, HC), 1.86−1.84 (m, 4H, HD), 1.61−1.55 (m, 4H, HE), 1.33 (bt, 6H, HF).

^{13}C NMR (CF_3COOD, 151 MHz, 298 K): δ (ppm) 133.2, 124.4, 41.9, 29.9, 19.3, 12.4.

HR-ESI-MS: calcd for $C_{32}H_{27}N_2O_4$ $[M + H]^+$, 503.19653; found, 503.19569.

2.2.2. N,N′-Bis(2-[2-Hydroxyethoxy]ethyl)perylene-3,4,9,10-tetracarboxylic Acid Bisimide (Per−OH). In a pressure-tight microwave tube under a nitrogen atmosphere, 100 mg of perylene-3,4,9,10-tetracarboxylic bisanhydride were suspended in 5 mL of dry DMF, and 2 equiv of 2-(2-aminoethoxyethanol) were added. The red suspension was sonicated for 5 min before heating under microwave irradiation at 50 W for 10 min. The heating was repeated for five cycles, with cooling intervals of 5 min. The maximum temperature was set at 200 °C. After cooling, the solution color turned dark red. The reaction was quenched by adding 50 mL of NaOH 1 M and stirring for 30 min (Scheme S2). The obtained precipitate was filtered, abundantly washed with water until neutral pH, and finally dried using a vacuum pump. The final product was obtained as a brown-red solid. Yield 59%.

^{1}H NMR (CF_3COOD, 600 MHz, 298 K): δ (ppm) 8.86 (dd, J = 7.0 Hz, 8H, HA and HB, AB system), 4.81 (t, J = 5.4 Hz, 4H, HD), 4.76−4.70 (m, 4H, HE), 4.33 (t, J = 5.4 Hz, 4H, HC), 4.29−4.24 (m, 4H, HF).

^{13}C NMR (CF_3COOD, 151 MHz, 298 K): δ (ppm) 132.6, 124.4, 68.6, 68.5, 66.9, 39.8.

MALDI-TOF: calcd for $C_{32}H_{27}N_2O_8$ $[M + H]^+$, 567.1767; found, 567.1732.

2.2.3. General Procedure for the Synthesis of PolyPer and Poly. All the equivalents are intended with respect to 1 equiv of HMDI. In a three-neck round-bottom flask, under nitrogen flux, polyethylene glycol (M_W = 1500 g mol^{-1}, Fluka, 0.5 equiv) was melted at 100 °C under mechanical stirring. **Per−OH** (0.01 equiv for **PolyPer1** and 0.05 equiv for **PolyPer5**, respectively) was added, and the mixture was stirred to disperse the chromophore homogeneously. Then, 0.5 equiv of 4,4-methylenebis(cyclohexyl isocyanate) (HMDI) and 0.001 equiv of 1,4-diazabicyclo[2.2.2]octane (DABCO) (solution 18 mM in acetonitrile) were added, and the stirring was maintained for 50 min, obtaining a dark viscous mixture. Finally, the remaining 0.5 equiv of HMDI and 0.5 equiv of 1,4-butanediol were added, and the mixture was stirred for about 30 min until it became too viscous to be efficiently stirred. The obtained polymer was poured onto an aluminum foil and dried under vacuum at 45 °C for one night. The final product was obtained as a dark red solid (Scheme S3). **Poly** was obtained by applying the same synthetic procedure without adding **Per−OH** (Scheme S4). The as-prepared materials were named according to their composition, where **Poly** stands for polyurethane, **Per** for *N*,*N*′-bis(2-[2-hydroxyethoxy]ethyl) perylene-3,4,9,10-tetracarboxylic acid bisimide, and numbers 1 and 5 correspond to 0.01 and 0.05 equiv of the dye, respectively. **Poly**, **PolyPer1**, and **PolyPer5** were purified by dissolution in THF (4% w/v solution) and filtration under vacuum. The filtered solution was then cast in a glass Petri dish for 24 h.

2.2.3.1. PolyPer5. ^{1}H NMR (DMSO-d_6, 400 MHz, 298 K): δ (ppm) 8.85 (d, J = 8.2 Hz, 0.2H, HB PER−OH), 8.51 (d, J = 7.9 Hz, 0.2H, HA PER−OH), 7.12, 6.97, 6.88, 6.71, 6.65 (s, 3H, NH), 4.59 (bt, 0.1H, terminal OH), 4.41 (t, 0.4H, J = 4.7 Hz, terminal OH), 4.37 (t, 0.4H, J = 5.1 Hz, terminal OH), 4.28 (t, 0.2H, J = 6.6 Hz, terminal OH), from 4.11 to 3.83 (m, 6H, OCH_2 PEG chain and butanediol chain, perylene chain), from 3.79−3.36 (m, 168H, PEG chain, perylene chain), 3.24−3.09 (m, 1H, CHN), from 1.87−077 (m, 44H, HMDI, CH_2CH_2 butanediol).

2.3. Film Preparation. The synthesized PUs (i.e., **PolyPer1** and **PolyPer5**) were blended with commercial **TPU** (poly[4,4′-methylenebis(phenyl-isocyanate)-*alt*-1,4-butanediol/di(propylene glycol)/poly caprolactone], purchased from Merck) to produce flexible and highly deformable films. Each synthesized PU was dissolved in THF (4% w/v solution) with commercial **TPU** (30:70 w/w) and cast in a Petri dish. After 24 h, the films were removed from the Petri dish and pressed in a compression molding apparatus (laboratory press, Carver C12, Carver Inc., Indiana USA) at 150 °C and 40 bar. The film produced using **PolyPer1** and **PolyPer5** contained a final concentration of covalently linked **Per−OH** of 0.15 and 0.78 wt %, respectively. These films were labeled **MC-0.15** and **MC-0.78**, where MC stands for "main chain" and refers to the covalent dye insertion in the synthesized PU main chain. Unfunctionalized **Poly**, **TPU**, and **Per** samples were also prepared by physical blending. **Poly** and **TPU** (30:70 w/w) were dissolved in THF (4% w/v solution), and proper amounts of **Per** were added to gain a final concentration of 0.15 and 0.78 wt %. Films were obtained by solvent casting and hot pressing, as previously described. These films were labeled **D-*x***, where D is the abbreviation of dispersed dye, and x (x = 0.15, 0.78) refers to the dye weight content. Films were stored at room temperature (RT) for at least 2 weeks before characterization to attain equilibrium crystallinity.

3. RESULTS AND DISCUSSION

3.1. Characterization of Synthesized Polyurethanes. Two different perylene-based chromophores were synthesized by applying a synthetic procedure adapted from the literature:[38] **Per**, bearing two unreactive butyl chains to be used as an additive in the preparation of dispersed dye samples (**D-*x***), and **Per−OH**, functionalized with two alkyl chains bearing hydroxyl groups at each terminus.

Both **Per** and **Per−OH** were fully characterized, and the corresponding ^{1}H- and HSQC NMR spectra are reported in Figures S1−S4. **Per−OH** was used for the preparation of **PolyPer1** and **PolyPer5**, together with PEG 1500, HMDI, and DABCO as a catalyst (Scheme S3). The quantity of chromophore **Per−OH** present in PolyPer1 was too low to allow its detection and quantification through ^{1}H NMR spectroscopy, while on the contrary, ^{1}H NMR analysis performed on **PolyPer5** confirmed the presence and expected quantity of **Per−OH** inside the polymer matrix (Figure S5). A similar PU not bearing the chromophore was synthesized and named **Poly** (Scheme S4).

The synthesized **PolyPer** and **Poly** are characterized by a number-average molecular weight (M_n) in the range 1960−2300 g mol^{-1} with a polydispersity $Đ \leq 2.0$ (Table S1). All of the prepared polymers have similar, relatively low molecular weights, thus indicating that the functionalization with **Per−OH** does not influence the synthetic process.

https://doi.org/10.1021/acsapm.3c02284
ACS Appl. Polym. Mater. 2024, 6, 669−680

DSC analyses were performed to evaluate how the different degrees of functionalization affect the thermal properties (Figure 1a). After polymer thermal histories are erased by melting and cooling at 10 °C min^{-1}, heating scans are analyzed. All synthesized PUs are semicrystalline with a glass-transition temperature (T_g) below RT. Above T_g, the DSC heating scan of **Poly** shows a narrow melting peak (T_m = 42 °C), which can be ascribed to PEG segments (pure PEG1500 shows T_m at ca. 45 °C[39]). The DSC traces of **PolyPer1** and **PolyPer5** similarly display a narrow melting peak that in these cases can also be attributed to the melting of PEG1500 segments. Calorimetric data of **PolyPer1**, **PolyPer5**, and **Poly** reported in Table S2 show that, upon increasing the amount of **Per−OH** in the main polymeric chain, both T_m and ΔH_m decrease. This result indicates that the presence of the chromophore in the main polymeric chain reduces the capability to crystallize, possibly due to the proximity of the chromophore to the PEG segments.

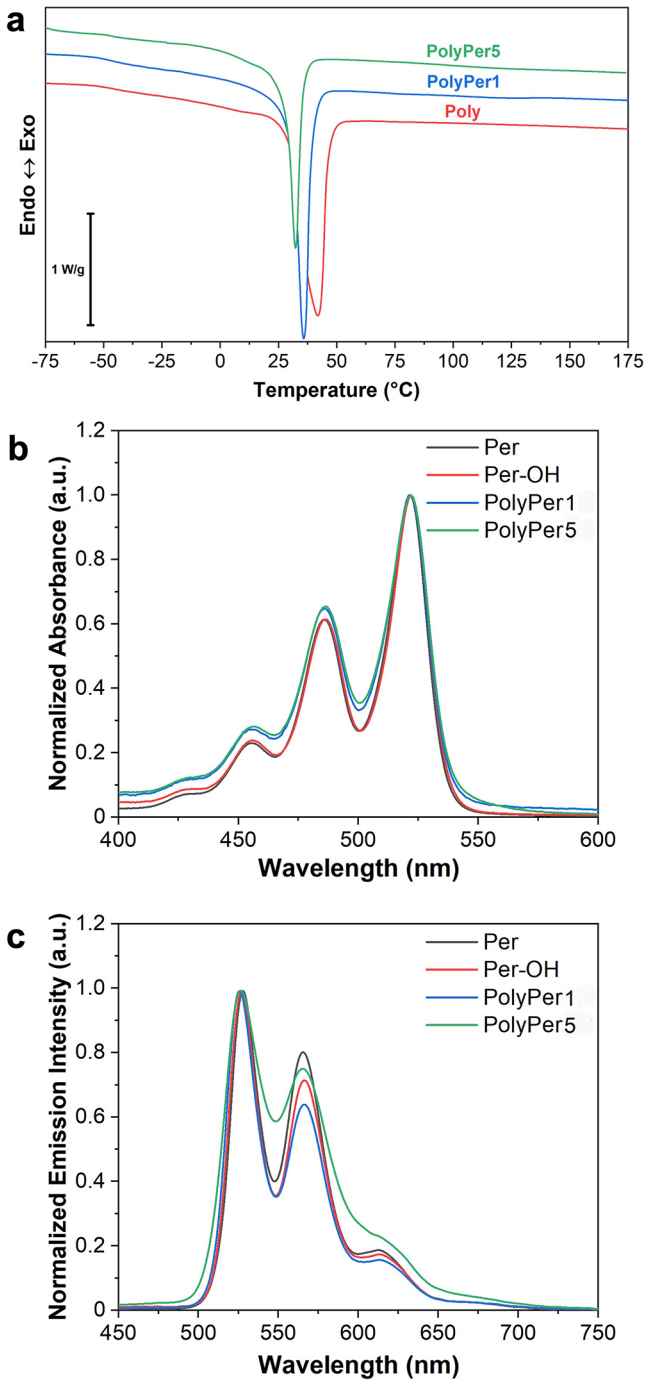

Figure 1. (a) DSC scans after controlled cooling at 10 °C min^{-1} of **Poly** (red), **PolyPer1** (blue), and **PolyPer5** (green); (b) UV−vis and (c) emission spectra (λ_{ex} = 485 nm) of THF solutions of **Per** (c = 15 μM, black), **Per−OH** (c = 15 μM, red), **PolyPer1** ($c_{Per-OH\ in\ the\ polymer}$ = 20 μM, blue), and **PolyPer5** ($c_{Per-OH\ in\ the\ polymer}$ = 20 μM, green).

The UV−vis absorption and fluorescence spectra of **Per**, **Per−OH**, **PolyPer1**, and **PolyPer5** solutions in THF were recorded (Figure 1b,c). The absorption spectra show an absorption maximum at 522 nm for all the materials under analysis, along with two higher vibronic transitions located at ∼486 and ∼456 nm, characteristic of perylene diimide (PDI) chromophores in solutions.[40,41] Additionally, the fluorescence spectra represent a mirror image of the absorption spectra and maintain the vibronic pattern accompanied by well-resolved fine structures, with the highest emission band at 526 nm for all of the materials under analysis. The similarities in the shapes and positions of dye and polymer absorption and emission spectra indicate that the different imide substituents do not significantly affect their photophysical properties. Furthermore, for both polymers, ground-state aggregation does not occur in solution.

3.2. Characterization of Per-Based Films. The synthesized polyurethanes were employed as additives of a high-MW commercial **TPU** presenting M_n = 93,410 g mol^{-1} and $Đ$ = 3.3 (Table S1), T_g below RT, and a broad melting between 100 and 180 °C[42] (Figure S6). **PolyPer1** and **PolyPer5** were added at 30 wt % concentration to **TPU** to prepare main chain (**MC**) compounds. Dispersed dye blends (**D**) were also produced by dispersing the free **Per** dye into a **TPU:Poly** 70:30 w/w blend.

The thermal behavior of both dispersed dye blends (**D**) and main chain systems (**MC**) is shown in Figure 2a,b, respectively, and calorimetric data are reported in Table S2. First heating scans of samples stored at RT for 2 weeks are analyzed in this case, this scan being representative of the starting condition for mechanochromic characterization. All films are semicrystalline and display a single T_g at ca. −45 °C, suggesting that **Poly**-based materials and **TPU** form a miscible blend. This result was further confirmed through DMTA analysis (Figure S7). Therefore, DSC and DMTA results suggest that, both in the dispersed dye blends and in the main chain systems, the chromophore, typically located in the amorphous phase, is closely in contact with both the blend components, without any preferential segregation. All samples show a broad melting endotherm in the range 20−55 °C, which can be attributed to the melting of PEG segments of the synthesized PU since plain **Per** does not show any transition in this temperature range (data not shown), and a weak and hardly measurable endothermal signal above 150 °C, ascribable to the melting of the commercial **TPU** (Table S3). Upon an increase in the amount of dispersed **Per** in **D** blends, the ΔH_m value of the PEG segments increases, indicating a possible nucleating action of **Per** aggregates. This behavior is not observed in **MC** systems, where, instead, upon increasing the amount of the chromophore in the main polymeric chain, a decrease in T_m is observed, as can be previously seen for the corresponding bulk materials. Notably, all the materials under analysis display similar mechanical properties, typical of common TPU, with a low Young's modulus and a high deformation at break, thus indicating that the presence of the chromophore either in the

https://doi.org/10.1021/acsapm.3c02284
ACS Appl. Polym. Mater. 2024, 6, 669−680

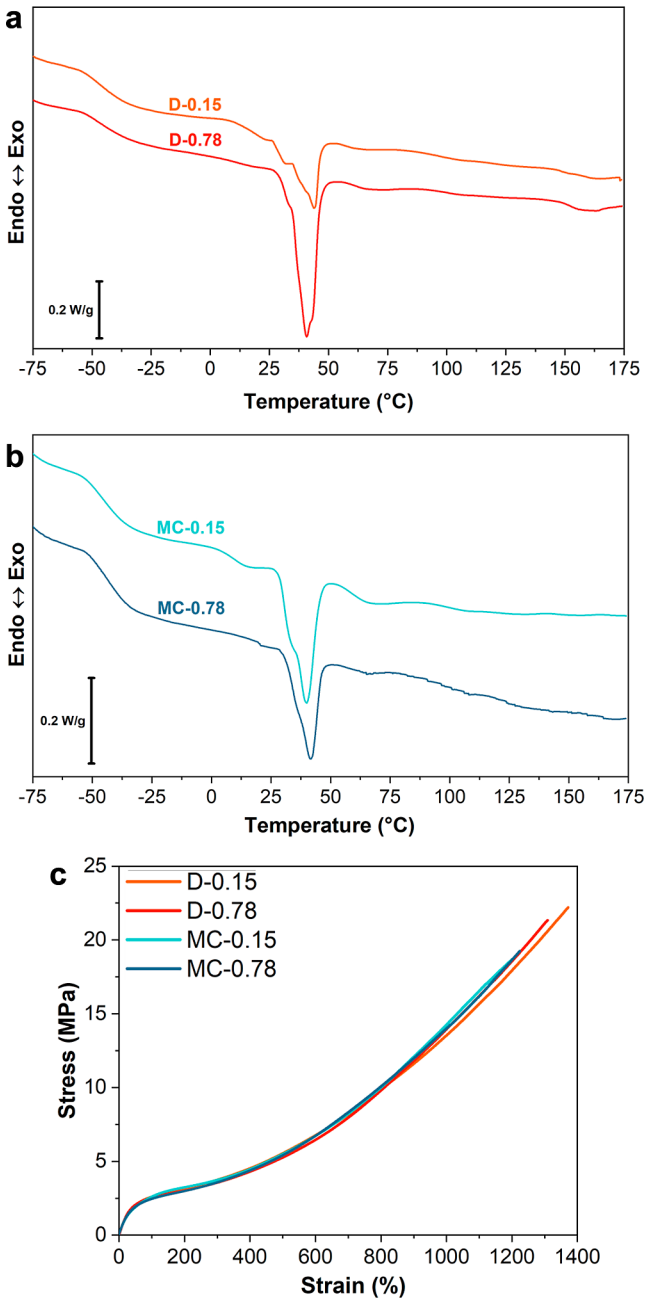

Figure 2. (a) DSC first heating scans of **D-0.15** (orange) and **D-0.78** (red); (b) DSC first heating scans of **MC-0.15** (cyan) and **MC-0.78** (blue); and (c) representative stress−strain curves of **D-0.15** (orange), **D-0.78** (red), **MC-0.15** (cyan), and **MC-0.78** (blue).

main polymeric chain or as a dispersed additive does not affect the mechanical properties of the material (Figure 2c and Table S4).[40,41]

When excited with UV light (λ_{ex} = 365 nm), **D** samples exhibit a bright red fluorescence, while **MC** samples display a green-yellow fluorescence (Figure S8). When compared with the monomeric emission of **Per**, these results indicate that a certain dye ground-state aggregation occurs in all of the investigated blends. Indeed, the fluorescence spectra of both **MC** and **D** samples under static conditions (Figure 3a), normalized at the aggregate's maximum emission (λ = 660 nm), show the emissions of both monomeric **Per** (λ = 568 nm) and **Per** aggregates. However, the contributions of these two emissions differ among the samples: in **MC** samples, the monomer emission dominates, presenting only a shoulder, while **D** samples show similar contributions, with the aggregation emission gaining weight as **Per** doping increases.

By comparing the ratio between the intensities at the monomer emission maximum [λ_{em}^{max} (monomer) = 568 nm, I_M] and at the aggregate emission maximum [λ_{em}^{max} (aggregate) = 660 nm, I_A] of **D** and **MC** samples, we can evaluate how the **Per** inclusion mode in the film affects the aggregation process: the lower this ratio (I_M/I_A), the higher will be the amount of **Per** aggregates. The values of the emission intensity ratio calculated for all of the **MC** and **D** samples are reported in Figure 3b. As expected, increasing the dye concentration favors aggregation (i.e., lower I_M/I_A). Moreover, it can be observed that **Per** aggregation occurs more easily in the dispersed system (**D**) rather than in the covalently linked one (**MC**) at the same dye concentration. This can be explained by the reduced mobility of the dye linked to the polymer chains compared with the dispersed ones.

3.3. Mechanochromic Properties of Per-Based Samples. After determining how the different concentrations of the chromophore and the different incorporation approaches (i.e., blended or bonded) affect the aggregation of **Per** chromophores in the investigated samples, we evaluated their mechanochromism by collecting their emission spectra in situ during stress−strain and stress relaxation experiments (Figure S9) under UV light excitation (λ_{ex} = 365 nm). Figures 4 and 5 report, for both **D** and **MC** samples, respectively, the normalized spectra obtained at different strains during stress−strain experiments.

A noticeable variation in the emission spectrum is observed upon stretching for **D** blends (Figure 4a,b). In **D-0.78**, the spectrum is initially dominated by the emission of the aggregates; as the deformation increases, the emission attributed to the **Per** monomer progressively increases (see the schematic representation of the **Per** disaggregation under stretching in Figure 4c). This behavior is also observed in the blend doped with a lower concentration of the dye, i.e., **D-0.15**, albeit the starting I_M/I_A is lower compared to **D-0.78**. These changes are visually apparent as the color shifts from orange to yellow in **D-0.15** and from red to orange in **D-0.78** (Figure 4a,b). In contrast, the **MC** samples show only a slight change in the emitted intensity (Figure 5a,b). This result can be attributed to the limited aggregation observed for **MC** systems (Figure 3b) which, in turn, leads to a minimal shift in the observed fluorescence color even at high strain (Figure 5c).

Then, the ratio between the intensity at the emission maximum of the monomer [I_M, with λ_{em}^{max} (monomer) = 568 nm] and that of the aggregate [I_A, with λ_{em}^{max} (aggregate) = 660 nm] was plotted versus the applied strain (Figure 6). For all of the samples, I_M/I_A increases with deformation, and a linear response is observed in the plastic deformation range. This indicates that rearrangements of the chains associated with disentanglement processes must occur to achieve disaggregation of the dyes in the **MC** and **D** samples. Notably, in **MC** samples, the trend of I_M/I_A appears to be highly scattered as a consequence of the small spectral variations recorded for these samples.

To better compare the mechanochromic performances of **D** and **MC** samples, the ratiometric emission intensity was plotted versus the strain in the linear mechanochromic range (i.e., strain comprised between 250 and 950%) and fitted with a linear function (Figure S10). By comparing the slopes of the

https://doi.org/10.1021/acsapm.3c02284
ACS Appl. Polym. Mater. 2024, 6, 669−680

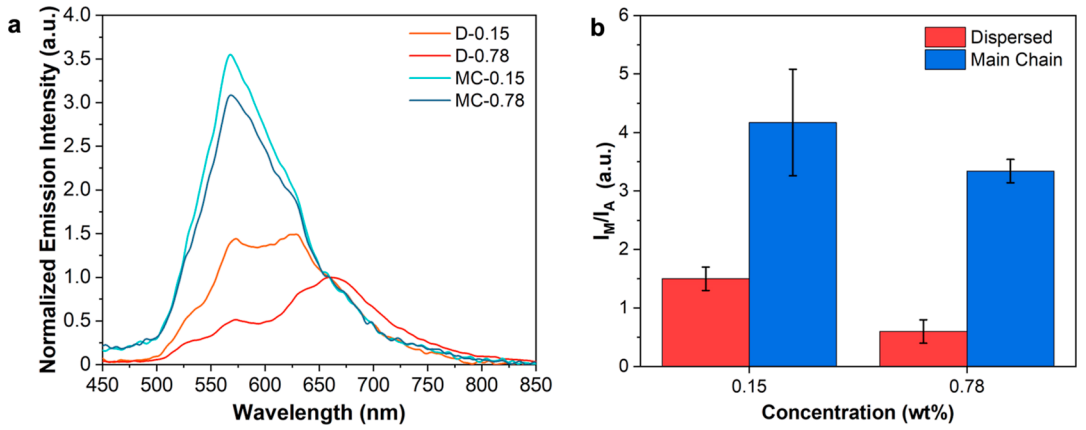

Figure 3. (a) Solid-state emission spectra of **D-0.15** (orange), **D-0.78** (red), **MC-0.15** (cyan), and **MC-0.78** (blue) and (b) I_M/I_A versus concentration of the chromophore for **D** (red) and **MC** (blue) samples. The results reported are averaged between three replicates for each sample.

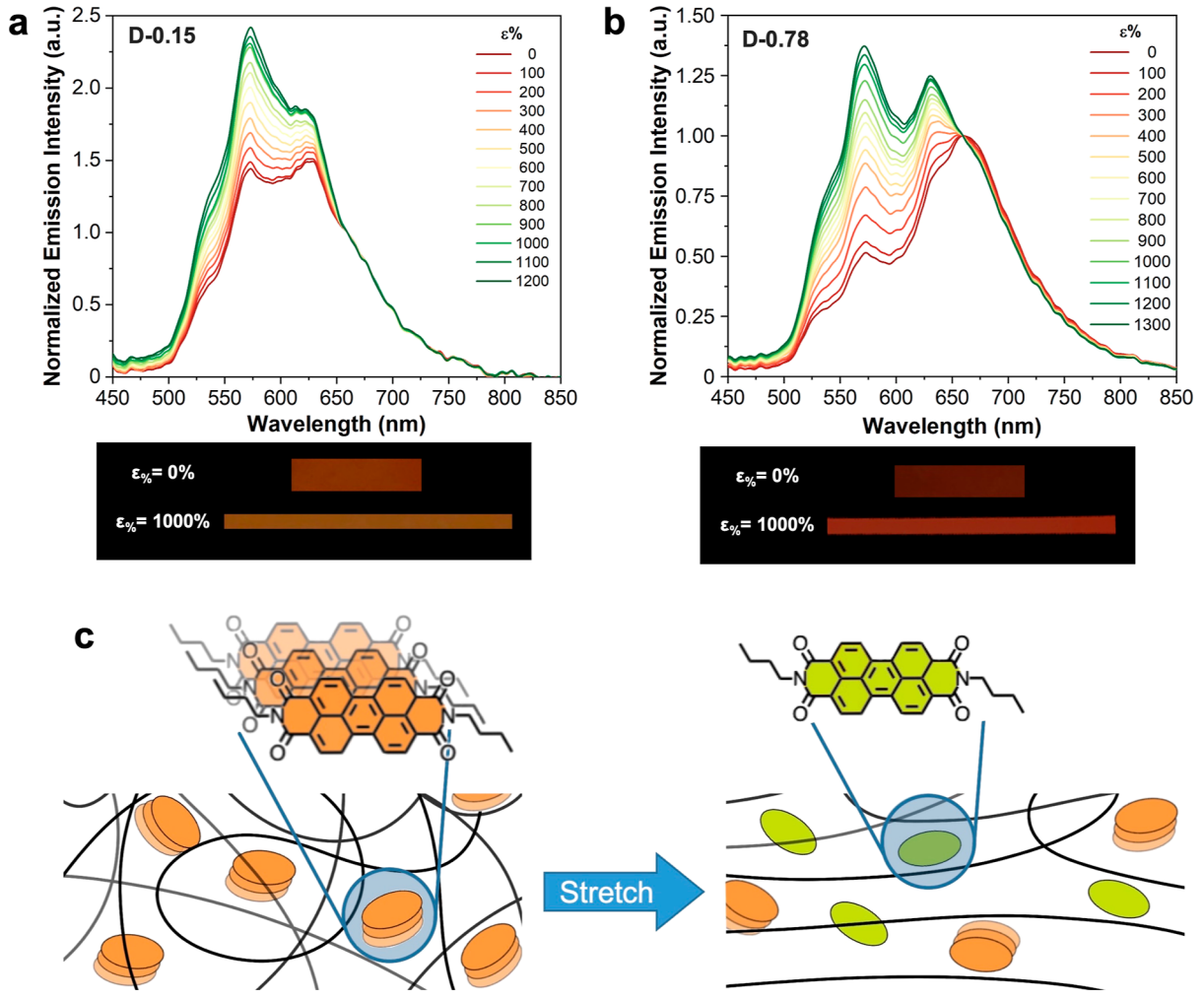

Figure 4. Solid-state emission spectra at increasing strains of (a) **D-0.15** and (b) **D-0.78** with the respective fluorescence images under UV light (λ_{ex} = 365 nm) of films at 0 and 1000% strains (ε) and (c) schematic representation of the mechanochromism in **D** blends.

linear fits reported in Table S5, for **D** blends, **D-0.15** displays a slightly higher mechanochromic sensitivity than **D-0.78**. This result might be attributed to the larger size of the aggregates in the sample at higher concentration. Similar results are obtained for **MC** systems, where the sample displaying the lowest concentration of dye (**MC-0.15**) shows the highest sensitivity.

When comparing **D** and **MC** systems, **MC** samples have slightly higher slopes for both concentrations, albeit, as previously discussed, the idle states present most of the dye in the monomeric form. This result does not contradict those reported in the literature for aggregachromic dyes, where mechanochromic polymers with the dye bound to the main polymeric chain generally display higher mechanochromic

https://doi.org/10.1021/acsapm.3c02284
ACS Appl. Polym. Mater. 2024, 6, 669−680

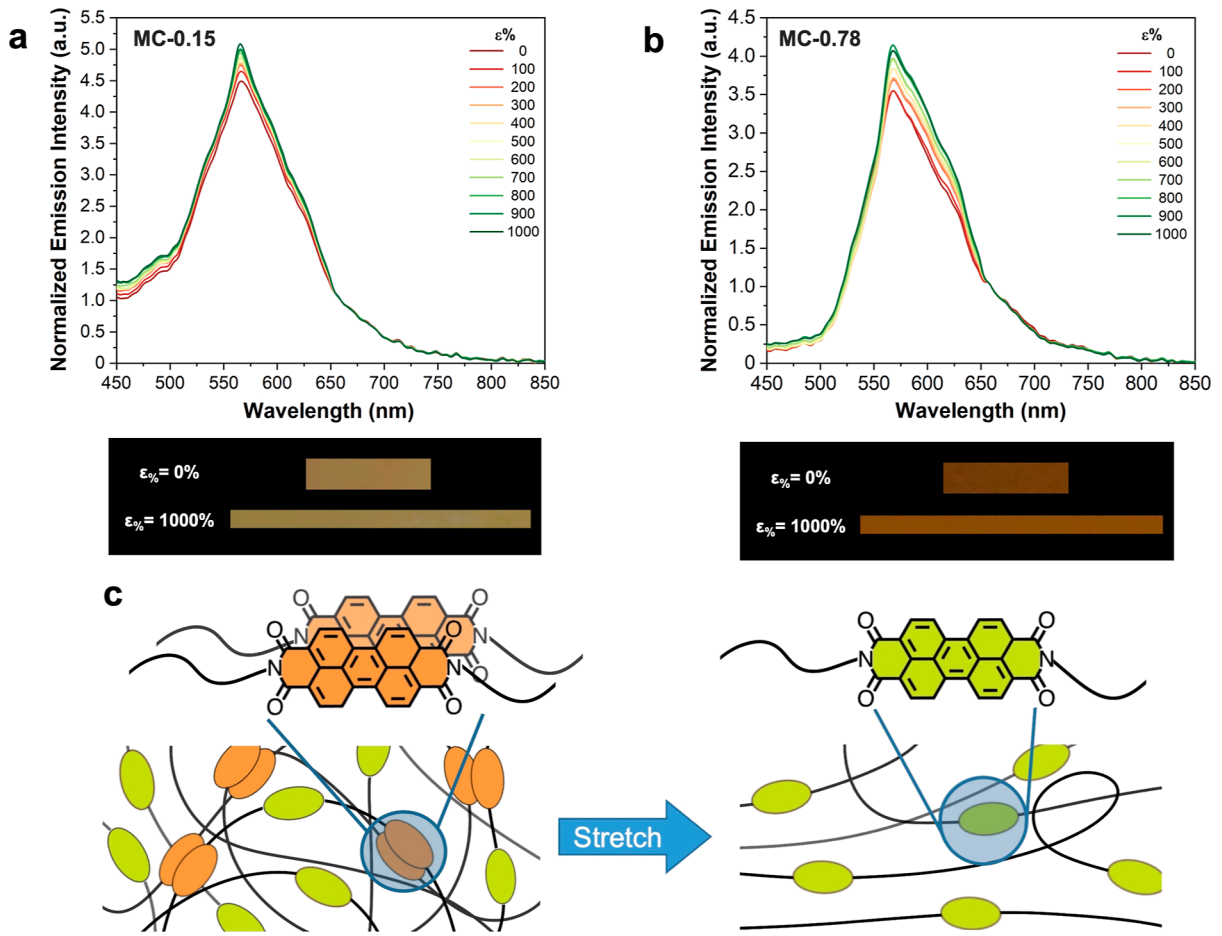

Figure 5. Solid-state emission spectra at different strains of (a) **MC-0.15** and (b) **MC-0.78** with the respective fluorescence images under UV light (λ_{ex} = 365 nm) of films at 0 and 1000% strains (ε) and (c) schematic representation of the mechanochromism in **MC** blends.

sensitivities than their dispersed dye counterparts.[23,27] It is worth noting that in the low range of dye concentration explored in this work, the amount of dye aggregates achieved in **MC** samples is insufficient to induce useful spectral variations under stretching (see Figure 5). Therefore, if a perceptible color variation is aimed, the direct comparison, performed by maintaining a constant dye concentration, demonstrates that, for polyurethanes, the blending approach is more effective in obtaining mechanochromic polymers than the bonding approach, at least in the low regime of dye concentration pursued with a focus on cost-effectiveness. Our finding is somehow supported by a study conducted by Weder and co-workers, wherein they reported mechanochromism when oligo(*p*-phenylenevinylene) derivatives were covalently incorporated into **TPU** at high concentration, specifically in the range 4−9 wt %. In contrast, for the blend, they used a lower dye concentration in the range of 0.1−0.4 wt %, but a direct comparison between blending and bonding at the same concentration was not reported by the authors.[31] In a recent paper, we addressed the comparison between blending and bonding, employing an elastomeric SEBS triblock copolymer.[23] In that study, we achieved a discernible and reversible mechanochromic response with a moderate dye concentration when the dye was covalently linked to the polymer chain. In contrast, achieving a detectable mechanochromism through physical dispersion necessitated a dye concentration 10 times higher. These findings contrast with those reported in the present work and could be achieved by exploiting the intrinsic phase separation of the SEBS copolymer which allowed the selective confinement of the dye units to the soft phase by covalently bonding the dye to the central block.

Samples **D-0.15** and **MC-0.15** were also subjected to deformation to 200% strain, followed by rapid unloading to 100% strain over four cycles, while the fluorescence intensity ratio, I_M/I_A, was continuously monitored (Figure 6e and f). Discarding the first cycle, which is affected by the Mullins effect (Figure S11), in the subsequent cycles, both samples experience dye disaggregation and reaggregation. Indeed, I_M/I_A displays a cyclic trend that synchronizes with the loading and unloading phases. However, in the **D-0.15** sample, the I_M/I_A curve exhibits a drift toward lower values. This implies that after each cycle, the degree of dye aggregation progressively increases, probably as a consequence of the fast and frequent chain rearrangements, facilitating the assembly of the highly mobile dye molecules. In **MC-0.15**, instead, the minimum and maximum values of I_M/I_A remain almost constant across the different cycles. This indicates that the extent of disaggregation and aggregation effectively mirrors the applied strain throughout the repeated deformation and relaxation steps.

Last, the stress relaxation behavior of **D** blends was assessed (Figure 7). For all the samples under analysis, the stress relaxation curves are those of common TPUs, with an initial rapid decrease in the stress, followed by a slower relaxation process.[43] For all samples, the stress applied was not fully relaxed at the end of the experiment (30 min). In both **D-0.15** and **D-0.78**, upon stress application, I_M/I_A increases (dis-

https://doi.org/10.1021/acsapm.3c02284
ACS Appl. Polym. Mater. 2024, 6, 669−680

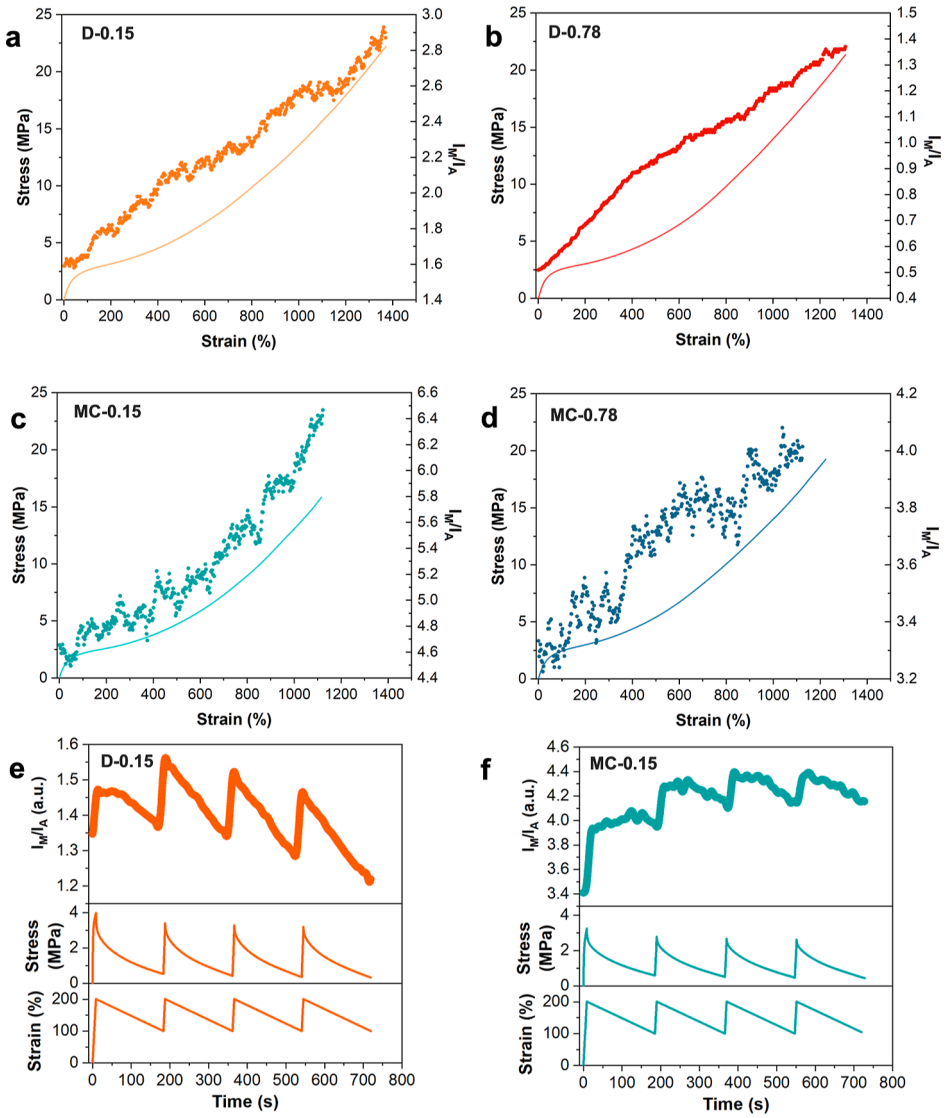

Figure 6. Stress−strain curves (solid lines) and I_M/I_A (dots) of (a) **D-0.15**, (b) **D-0.78**, (c) **MC-0.15**, and (d) **MC-0.78**. The results reported are averaged among the three samples. Cyclic loading−unloading experiments performed on (e) **D-0.15** and (f) **MC-0.15** over four cycles between 100 and 200% strain: stress, strain, and I_M/I_A as a function of time.

aggregation phase, Figure 7i), similar to what was observed in stress−strain experiments. After this initial disaggregation phase, which is concomitant with the strain phase of the experiment, a progressive increase of I_M/I_A is observed, indicating that disaggregation of the material still occurs during the first phase of stress relaxation. This phase lasts ca. 130 s for both **D-0.15** and **D-0.78** and is followed by a plateau region, which lasts ca. 280 s for both blends (Figure 7ii). Surprisingly, I_M/I_A decreases after this second phase, meaning that the dye monomers reaggregate (aggregation phase, Figure 7iii). In **D-0.15**, the final I_M/I_A is higher than the value measured at the idle state (1.216 vs 1.250), meaning that the initial dye aggregation degree is not reached after 30 min of stress relaxation; in contrast, for **D-0.78**, the final I_M/I_A measured is lower than the initial value (3.538 vs 3.294, Table S6).

The mechanochromism during stress relaxation tests in the dispersed dye system can be justified by considering the microstructural rearrangements during stress relaxation, as depicted in Figure 8a for the **D-0.15** sample. When **TPU** is stretched, the dye disaggregates (Figure 8a(i)), while the polymeric network is deformed, thus changing its conformation from the highly entropically favored random coil conformation to a more aligned conformation, leading to a decrease in entropy that is rapidly recovered when the strain is fixed. Since this driving force does not affect the dispersed dyes, they will retain their inertial motion longer, with no driving force for reaggregation (plateau region, Figure 8a(ii)). Reaggregation of the dyes will then occur, possibly triggered by the decrease in free volume induced by strain-induced crystallization, thus leading to the observed decrease in I_M/I_A (Figure 8a(iii)). This hypothesis is well supported by analysis of ΔH_m before and after the stress relaxation experiment (Table S6), which clearly shows that the material undergoes a strain-induced crystallization, with the final ΔH_m being comparable for all of the blends under analysis. This effect is more evident upon increasing the dye concentration, with the **D-0.78** sample reaching a lower I_M/I_A at the end of the experiment than at the starting one.

https://doi.org/10.1021/acsapm.3c02284
ACS Appl. Polym. Mater. 2024, 6, 669−680

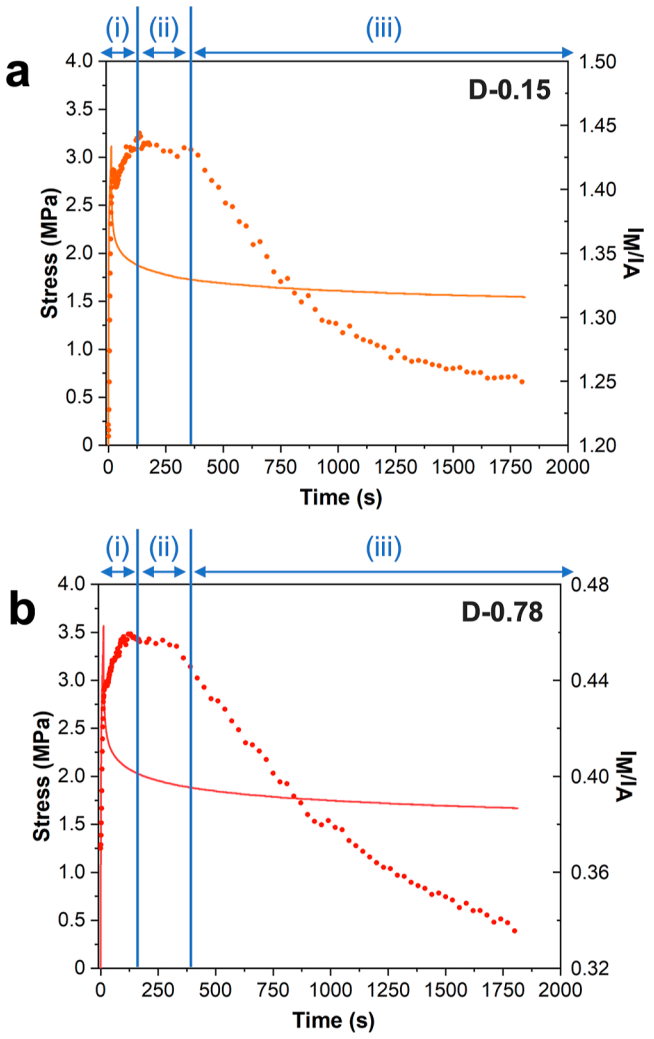

Figure 7. Stress relaxation curves (solid lines) and I_M/I_A (dots) of (a) **D-0.15** and (b) **D-0.78**. The trend of I_M/I_A over time can be divided into three regions: an initial disaggregation phase (i), followed by a plateau region (ii), and a reaggregation phase (iii).

Stress relaxation analysis was also performed on **MC-0.15** (Figure 8b) to compare the response of **MC** and **D** systems at the same concentration. Also for **MC-0.15**, the stress relaxation response is that of common TPUs, with an initial rapid decrease in the stress, followed by a slower relaxation process without a complete relaxation of the applied stress at the end of the experiment. We observe the presence of an initial disaggregation phase (Figure 8b(i)), immediately followed by an assembly phase (Figure 8b(iii)), with a final aggregation degree higher than that in the idle state. As can be seen for **D-0.15**, **MC-0.15** shows a delay between the mechanical stress relaxation phase and the end of the mechanochromic disaggregation (ca. 170 s for **MC-0.15** and ca. 120 s for **D-0.15**); however, for this blend, no plateau region is observed, and the I_M/I_A ratio in **MC-0.15** better follows the mechanical stress relaxation than the dispersed dye blend at the same concentration. **MC-0.15** also undergoes strain-induced crystallization, but in this case, the increment of ΔH_m is lower than what was observed for **D-0.15** (Table S6). Therefore, this moderate increase in the number of crystal domains, justified by the lower crystallization capacity of the **MC** sample due to the presence of the chromophore in the chain, hardly explains the high final aggregation degree achieved by **Per** units at the end of the experiment. To justify this behavior, Bergström's constitutive model for hysteresis and stress relaxation in elastomers[43] can be considered. According to this model,[43] stress relaxation in elastomers is mainly affected by the reptation and Brownian displacement of macromolecules that are "elastically inactive", namely, chains that can be highly stretched during fast applied macroscopic deformation but with loose connectivity to the main load-bearing chains. In our **MC** sample, being the two components miscible in the amorphous phase, the chains of **PolyPer** are entangled with the chains of commercial **TPU** and subjected together to deformation. However, **PolyPer** chains, being shorter in length, are unlikely involved in more than one physical cross-link points. For these reasons, they can be considered to be elastically inactive chains, while **TPU** is the load-bearing component. Based on this assumption, the mechanochromism

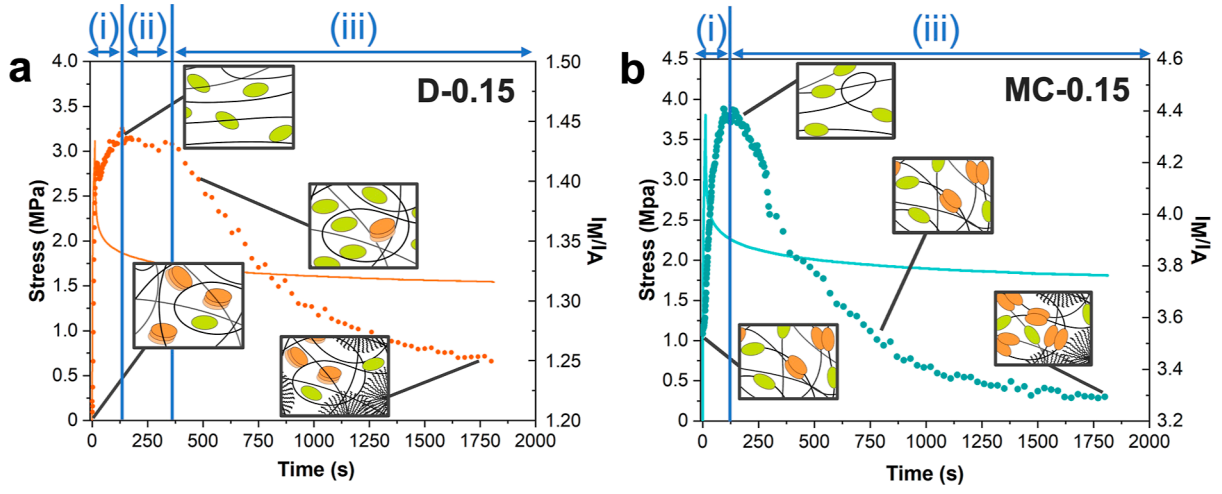

Figure 8. Stress relaxation curves (solid lines) and I_M/I_A (dots) of (a) **D-0.15** and (b) **MC-0.15**. For the **D-0.15** sample, the trend of I_M/I_A during time can be divided into three regions: an initial disaggregation phase (i), followed by a plateau region, (ii) and a reaggregation phase (iii); for the **MC-0.15** sample, the trend of I_M/I_A during time shows only two regions: an initial disaggregation phase (i), followed by a reaggregation phase (iii), with no plateau region. The sketches provide a schematic representation of how the dye aggregation state changes during the stress relaxation experiment.

https://doi.org/10.1021/acsapm.3c02284
ACS Appl. Polym. Mater. 2024, 6, 669−680

of the **MC** sample during the stress relaxation test can be explained as follows: the initial fast stress relaxation process, which impacts mainly the unfunctionalized **TPU**, is followed by a delayed rearrangement of the polymeric chains containing the chromophore, which promotes the dye reaggregation.

Overall, stress relaxation experiments show that even if the number of aggregates formed with the bonding approach is significantly lower compared to the blending one, the **MC** sample allows for a full recovery of the initial aggregates during stress relaxation, in contrast to the **D** sample in which aggregates are not recovered during relaxation of the stress and their rupture is irreversible in this phase. In a second phase, the phenomenon of strain-induced crystallization results, in both **MC** and **D** approaches, in the formation of further aggregates as a consequence of the dye concentration in the remaining amorphous phase.

4. CONCLUSIONS

The mechanochromic performances of TPUs containing a perylene diimide derivative (**Per**), either covalently linked to the main polymeric chains or simply used as an additive, were evaluated to determine the effects of the two incorporation approaches. To this purpose, polyurethanes (**PU**) covalently functionalized with a perylene diimide derivative in different mol % were synthesized and blended with a commercial **TPU** (**MC** samples). Parallelly, blends of commercial **TPU** and unfunctionalized synthetic **PU** were prepared and doped with different concentrations of dispersed perylene dye (**D** samples). Thermal characterization of the materials proved that dye aggregates favor polymer crystallization in dispersed blends. Conversely, increasing the chromophore concentration in the main chains decreases ΔH_m, possibly because the chromophore is linked to the crystallizing segments of the synthesized **PU**. However, no significant differences were observed in the mechanical behavior of these materials. As expected, spectroscopic characterization at rest highlights that the relative emission intensities of the dyes in monomeric and aggregate forms strongly depend on the dye concentration for both the **D** and **MC** systems. However, at the same dye concentration, the aggregate emission in **MC** samples is significantly lower compared to that in **D** counterparts, probably due to a reduced mobility and conformational freedom of the dyes linked to the polymer chains compared to the dispersed ones. For this reason, under uniaxial tensile strain, **D** samples display a higher emission color variation, which is appreciable by the naked eye. These results prove that covalently functionalizing the dye to the main polymeric chain does not significantly improve the mechanochromic response under uniaxial strain for this type of material compared to simpler and more cost-effective blending approach, at least in the low concentration regime of the dye investigated in the present work. In stress relaxation experiments and in cyclic loading−unloading experiments, conversely, a comparison between dispersed and main chain systems at the same dye concentration highlighted that the latter showed an improved correspondence between the mechanical data and the mechanochromic response. Considering the literature on this topic, it can be concluded that the polymeric matrix plays a key role in determining the aggregation state of the dye, and both the covalent approach and the physical blend can be advantageous depending on the type of the polymer. However, as for the mechanoresponse, the results of cyclic deformation and stress relaxation experiments corroborate previous findings stating that the covalent bonding of the dye elicits a better force-dependent fluorescence response than the physical dispersion. Overall, these results highlight the potential of mechanochromic elastomers based on physical dispersions of aggregachromic dyes, providing a more straightforward and cheaper synthetic route than covalent incorporation while still retaining high sensitivity and visibly discerning color changes. Due to its improved responsiveness to stress relaxation phenomena, the covalent incorporation of dyes remains an attractive alternative for damage detection.

■ ASSOCIATED CONTENT

Supporting Information

The Supporting Information is available free of charge at https://pubs.acs.org/doi/10.1021/acsapm.3c02284.

Additional characterization details on the synthesis, NMR spectroscopy, MS spectrometry, GPC chromatograms, mechanochromic characterization setup, and TPU's emission spectra (PDF)

■ AUTHOR INFORMATION

Corresponding Author

Chiara Gualandi − *Department of Chemistry "Giacomo Ciamician" and INSTM UdR of Bologna, University of Bologna, 40126 Bologna, Italy; Health Sciences & Technologies (HST) CIRI, University of Bologna, 40064 Bologna, Italy; Interdepartmental Center for Industrial Research on Advanced Applications in Mechanical Engineering and Materials Technology, CIRI-MAM, University of Bologna, 40136 Bologna, Italy;* orcid.org/0000-0002-2020-1892; Email: c.gualandi@unibo.it

Authors

Emma Contini − *Department of Chemistry "Giacomo Ciamician" and INSTM UdR of Bologna, University of Bologna, 40126 Bologna, Italy*

Valentina Antonia Dini − *Department of Chemistry "Giacomo Ciamician" and INSTM UdR of Bologna, University of Bologna, 40126 Bologna, Italy*

Andrea Rozzi − *Department of Chemistry, Life Sciences and Environmental Sustainability and INSTM UdR Parma, University of Parma, Parma 43123, Italy*

Damiano Genovese − *Department of Chemistry "Giacomo Ciamician" and INSTM UdR of Bologna, University of Bologna, 40126 Bologna, Italy;* orcid.org/0000-0002-4389-7247

Nelsi Zaccheroni − *Department of Chemistry "Giacomo Ciamician" and INSTM UdR of Bologna, University of Bologna, 40126 Bologna, Italy*

Alessandro Pedrini − *Department of Chemistry, Life Sciences and Environmental Sustainability and INSTM UdR Parma, University of Parma, Parma 43123, Italy*

Enrico Dalcanale − *Department of Chemistry, Life Sciences and Environmental Sustainability and INSTM UdR Parma, University of Parma, Parma 43123, Italy;* orcid.org/0000-0001-6964-788X

Roberta Pinalli − *Department of Chemistry, Life Sciences and Environmental Sustainability and INSTM UdR Parma, University of Parma, Parma 43123, Italy;* orcid.org/0000-0002-0000-8980

Complete contact information is available at: https://pubs.acs.org/10.1021/acsapm.3c02284

Author Contributions

The manuscript was written through contributions of all authors. All authors have given approval to the final version of the manuscript.

Funding

This work was supported by MIUR-PRIN 20179BJNA2. This work benefited from the equipment and framework of the COMP-HUB Initiative, funded by the Departments of Excellence program of the Italian Ministry for Education, University and Research (MIUR, 2018−2022).

Notes

The authors declare no competing financial interest.

■ ACKNOWLEDGMENTS

The Centro Misure G. Casnati (CIM) is acknowledged for the use of NMR and MS facilities.

■ REFERENCES

(1) Caruso, M. M.; Davis, D. A.; Shen, Q.; Odom, S. A.; Sottos, N. R.; White, S. R.; Moore, J. S. Mechanically-Induced Chemical Changes in Polymeric Materials. *Chem. Rev.* **2009**, *109* (11), 5755−5798.

(2) Simon, Y. C.; Craig, S. L. *Mechanochemistry in Materials*, 1st ed.; Royal Society of Chemistry, 2017.

(3) Xu, J.; Chi, Z. *Mechanochromic Fluorescent Materials: Phenomena, Materials and Applications*; Xu, J., Chi, Z., Eds.; *Smart Materials Series*; Royal Society of Chemistry: Cambridge, 2014.10.1039/9781782623229.

(4) Urban, M. W. *Handbook of Stimuli-Responsive Materials*; WILEY-VCH Verlag GmbH & Co. KGaA: Weinheim, 2011.

(5) Lefebvre, E.; Piselli, A.; Faucheu, J.; Delafosse, D.; Del Curto, B. Smart Materials: Development of New Sensory Experiences through Stimuli Responsive Materials. *5th STS Italia Conference A Matter of Design: Making Society through Science and Technology*, 2014; pp 367−382.

(6) Ciardelli, F.; Ruggeri, G.; Pucci, A. Dye-Containing Polymers: Methods for Preparation of Mechanochromic Materials. *Chem. Soc. Rev.* **2013**, *42* (3), 857−870.

(7) Calvino, C.; Neumann, L.; Weder, C.; Schrettl, S. Approaches to Polymeric Mechanochromic Materials. *J. Polym. Sci., Part A: Polym. Chem.* **2017**, *55* (4), 640−652.

(8) He, S.; Stratigaki, M.; Centeno, S. P.; Dreuw, A.; Göstl, R. Tailoring the Properties of Optical Force Probes for Polymer Mechanochemistry. *Chem.—Eur. J.* **2021**, *27* (64), 15889−15897.

(9) Traeger, H.; Kiebala, D. J.; Weder, C.; Schrettl, S. From Molecules to Polymers—Harnessing Inter- and Intramolecular Interactions to Create Mechanochromic Materials. *Macromol. Rapid Commun.* **2021**, *42* (1), 1−32.

(10) Davis, D. A.; Hamilton, A.; Yang, J.; Cremar, L. D.; Van Gough, D.; Potisek, S. L.; Ong, M. T.; Braun, P. V.; Martínez, T. J.; White, S. R.; Moore, J. S.; Sottos, N. R. Force-Induced Activation of Covalent Bonds in Mechanoresponsive Polymeric Materials. *Nature* **2009**, *459* (7243), 68−72.

(11) Raisch, M.; Genovese, D.; Zaccheroni, N.; Schmidt, S. B.; Focarete, M. L.; Sommer, M.; Gualandi, C. Highly Sensitive, Anisotropic, and Reversible Stress/Strain-Sensors from Mechanochromic Nanofiber Composites. *Adv. Mater.* **2018**, *30* (39), 1802813.

(12) Lee, C. K.; Beiermann, B. A.; Silberstein, M. N.; Wang, J.; Moore, J. S.; Sottos, N. R.; Braun, P. V. Exploiting Force Sensitive Spiropyrans as Molecular Level Probes. *Macromolecules* **2013**, *46* (10), 3746−3752.

(13) Clough, J. M.; Van Der Gucht, J.; Sijbesma, R. P. Mechanoluminescent Imaging of Osmotic Stress-Induced Damage in a Glassy Polymer Network. *Macromolecules* **2017**, *50* (5), 2043−2053.

(14) Yan, C.; Yang, F.; Wu, M.; Yuan, Y.; Chen, F.; Chen, Y. Phase-Locked Dynamic and Mechanoresponsive Bonds Design toward Robust and Mechanoluminescent Self-Healing Polyurethanes: A Microscopic View of Self-Healing Behaviors. *Macromolecules* **2019**, *52* (23), 9376−9382.

(15) Yuan, W.; Yuan, Y.; Yang, F.; Wu, M.; Chen, Y. Improving Mechanoluminescent Sensitivity of 1,2-Dioxetane-Containing Thermoplastic Polyurethanes by Controlling Energy Transfer across Polymer Chains. *Macromolecules* **2018**, *51* (21), 9019−9025.

(16) Imato, K.; Kanehara, T.; Ohishi, T.; Nishihara, M.; Yajima, H.; Ito, M.; Takahara, A.; Otsuka, H. Mechanochromic Dynamic Covalent Elastomers: Quantitative Stress Evaluation and Autonomous Recovery. *ACS Macro Lett.* **2015**, *4* (11), 1307−1311.

(17) Imato, K.; Irie, A.; Kosuge, T.; Ohishi, T.; Nishihara, M.; Takahara, A.; Otsuka, H. Mechanophores with a Reversible Radical System and Freezing-Induced Mechanochemistry in Polymer Solutions and Gels. *Angew. Chem.* **2015**, *127* (21), 6266−6270.

(18) Imato, K.; Natterodt, J. C.; Sapkota, J.; Goseki, R.; Weder, C.; Takahara, A.; Otsuka, H. Dynamic Covalent Diarylbibenzofuranone-Modified Nanocellulose: Mechanochromic Behaviour and Application in Self-Healing Polymer Composites. *Polym. Chem.* **2017**, *8* (13), 2115−2122.

(19) Wang, L.; Zhou, W.; Tang, Q.; Yang, H.; Zhou, Q.; Zhang, X. Rhodamine-Functionalized Mechanochromic and Mechanofluorescent Hydrogels with Enhanced Mechanoresponsive Sensitivity. *Polymers* **2018**, *10* (9), 994.

(20) Wang, L. J.; Yang, K. X.; Zhou, Q.; Yang, H. Y.; He, J. Q.; Zhang, X. Y. Rhodamine Mechanophore Functionalized Mechanochromic Double Network Hydrogels with High Sensitivity to Stress. *Chin. J. Polym. Sci.* **2020**, *38* (1), 24−36.

(21) Osler, S. K.; McFadden, M. E.; Robb, M. J. Comparison of the Reactivity of Isomeric 2H- and 3H-Naphthopyran Mechanophores. *J. Polym. Sci.* **2021**, *59* (21), 2537−2544.

(22) Qi, Q.; Sekhon, G.; Chandradat, R.; Ofodum, N. M.; Shen, T.; Scrimgeour, J.; Joy, M.; Wriedt, M.; Jayathirtha, M.; Darie, C. C.; Shipp, D. A.; Liu, X.; Lu, X. Force-Induced Near-Infrared Chromism of Mechanophore-Linked Polymers. *J. Am. Chem. Soc.* **2021**, *143* (42), 17337−17343.

(23) Micheletti, C.; Dini, V. A.; Carlotti, M.; Fuso, F.; Genovese, D.; Zaccheroni, N.; Gualandi, C.; Pucci, A. Blending or Bonding? Mechanochromism of an Aggregachromic Mechanophore in a Thermoplastic Elastomer. *ACS Appl. Polym. Mater.* **2023**, *5* (2), 1545−1555.

(24) Willis-Fox, N.; Watchorn-Rokutan, E.; Rognin, E.; Daly, R. Technology Pull: Scale-up of Polymeric Mechanochemical Force Sensors. *Trends Chem.* **2023**, *05* (06), 415−431.

(25) Kiebala, D. J.; Fan, Z.; Calvino, C.; Fehlmann, L.; Schrettl, S.; Weder, C. Mechanoresponsive Elastomers Made with Excimer-Forming Telechelics. *Org. Mater.* **2020**, *02* (04), 313−322.

(26) Calvino, C.; Sagara, Y.; Buclin, V.; Haehnel, A. P.; del Prado, A.; Aeby, C.; Simon, Y. C.; Schrettl, S.; Weder, C. Mechanoresponsive, Luminescent Polymer Blends Based on an Excimer-Forming Telechelic Macromolecule. *Macromol. Rapid Commun.* **2019**, *40* (1), 1−8.

(27) Traeger, H.; Sagara, Y.; Kiebala, D. J.; Schrettl, S.; Weder, C. Folded Perylene Diimide Loops as Mechanoresponsive Motifs. *Angew. Chem.* **2021**, *133* (29), 16327−16335.

(28) Traeger, H.; Sagara, Y.; Berrocal, J. A.; Schrettl, S.; Weder, C. Strain-Correlated Mechanochromism in Different Polyurethanes Featuring a Supramolecular Mechanophore. *Polym. Chem.* **2022**, *13* (19), 2860−2869.

(29) Das, A. D.; Mannoni, G.; Früh, A. E.; Orsi, D.; Pinalli, R.; Dalcanale, E. Damage-Reporting Carbon Fiber Epoxy Composites. *ACS Appl. Polym. Mater.* **2019**, *1* (11), 2990−2997.

(30) Löwe, C.; Weder, C. Oligo(p-Phenylene Vinylene) Excimers as Molecular Probes: Deformation-Induced Color Changes in Photoluminescent Polymer Blends. *Adv. Mater.* **2002**, *14* (22), 1625−1629.

(31) Crenshaw, B. R.; Weder, C. Self-Assessing Photoluminescent Polyurethanes. *Macromolecules* **2006**, *39* (26), 9581−9589.

https://doi.org/10.1021/acsapm.3c02284
ACS Appl. Polym. Mater. 2024, 6, 669−680

(32) Crenshaw, B. R.; Weder, C. Deformation-Induced Color Changes in Melt-Processed Photoluminescent Polymer Blends. *Chem. Mater.* **2003**, *15* (25), 4717−4724.
(33) Rossi, N. A. A.; Duplock, E. J.; Meegan, J.; Roberts, D. R. T.; Murphy, J. J.; Patel, M.; Holder, S. J. Synthesis and Characterisation of Pyrene-Labelled Polydimethylsiloxane Networks: Towards the In Situ Detection of Strain in Silicone Elastomers. *J. Mater. Chem.* **2009**, *19* (41), 7674−7686.
(34) Donati, F.; Pucci, A.; Cappelli, C.; Mennucci, B.; Ruggeri, G. Modulation of the Optical Response of Polyethylene Films Containing Luminescent Perylene Chromophores. *J. Phys. Chem. B* **2008**, *112* (12), 3668−3679.
(35) Micheletti, C.; Minei, P.; Carlotti, M.; Mattoli, V.; Muniz-Miranda, F.; Perfetto, A.; Ciofini, I.; Adamo, C.; Ruggeri, G.; Pucci, A. Mechanochromic LLDPE Films Doped with NIR Reflective Paliogen Black. *Macromol. Rapid Commun.* **2021**, *42* (1), 2000426.
(36) Pucci, A.; Bertoldo, M.; Bronco, S. Luminescent Bis-(Benzoxazolyl)Stilbene as a Molecular Probe for Poly(Propylene) Film Deformation. *Macromol. Rapid Commun.* **2005**, *26* (13), 1043−1048.
(37) *ASTM D1708-18. Standard Test Method for Tensile Properties of Plastics by Use of Microtensile Specimens*, 2018..
(38) Rigodanza, F.; Tenori, E.; Bonasera, A.; Syrgiannis, Z.; Prato, M. Fast and Efficient Microwave-Assisted Synthesis of Perylenebisimides. *Eur. J. Org. Chem.* **2015**, *2015* (23), 5060−5063.
(39) Hamad, F. A.; Egelle, E.; Cummings, K.; Russell, P. Investigation of the Melting Process of Polyethylene Glycol 1500 (PEG 1500) in a Rectagular Enclosure. *Int. J. Heat Mass Transfer* **2017**, *114*, 1234−1247.
(40) Mauck, C. M.; Young, R. M.; Wasielewski, M. R. Characterization of Excimer Relaxation via Femtosecond Shortwave and Mid-Infrared Spectroscopy. *J. Phys. Chem. A* **2017**, *121* (4), 784−792.
(41) Margulies, E. A.; Shoer, L. E.; Eaton, S. W.; Wasielewski, M. R. Excimer Formation in Cofacial and Slip-Stacked Perylene-3,4:9,10-Bis(Dicarboximide) Dimers on a Redox-Inactive Triptycene Scaffold. *Phys. Chem. Chem. Phys.* **2014**, *16* (43), 23735−23742.
(42) Gotti, C.; Sensini, A.; Fornaia, G.; Gualandi, C.; Zucchelli, A.; Focarete, M. L. Biomimetic Hierarchically Arranged Nanofibrous Structures Resembling the Architecture and the Passive Mechanical Properties of Skeletal Muscles: A Step Forward Toward Artificial Muscle. *Front. Bioeng. Biotechnol.* **2020**, *8*, 767.
(43) Bergström, J. S.; Boyce, M. C. Constitutive Modeling of the Large Strain Time-Dependent Behavior of Elastomers. *J. Mech. Phys. Solids* **1998**, *46* (5), 931−954.

https://doi.org/10.1021/acsapm.3c02284
ACS Appl. Polym. Mater. 2024, 6, 669−680

Comparative mechanochromic performance of perylene diimide-doped polyurethanes: blending vs bonding

Supporting Information

Emma Contini[1], Valentina Antonia Dini[1], Andrea Rozzi[2], Damiano Genovese[1], Nelsi Zaccheroni[1], Alessandro Pedrini[2], Enrico Dalcanale[2], Roberta Pinalli[2], Chiara Gualandi[1,3,4]*

[1]Department of Chemistry "Giacomo Ciamician" and INSTM UdR of Bologna, University of Bologna, Via Selmi 2, 40126 Bologna, Italy

[2]Department of Chemistry, Life Sciences and Environmental Sustainability and INSTM UdR Parma, University of Parma, Parco Area delle Scienze 17/A, Parma 43123, Italy

[3]Health Sciences & Technologies (HST) CIRI, University of Bologna, Via Tolara di Sopra 41/E, 40064 Ozzano Emilia Bologna, Italy

[4]Interdepartmental Center for Industrial Research on Advanced Applications in Mechanical Engineering and Materials Technology, CIRI-MAM, University of Bologna, Viale Risorgimento 2, 40136 Bologna, Italy

* Corresponding Author: Prof. Chiara Gualandi, e-mail: c.gualandi@unibo.it

1. Synthetic Schemes

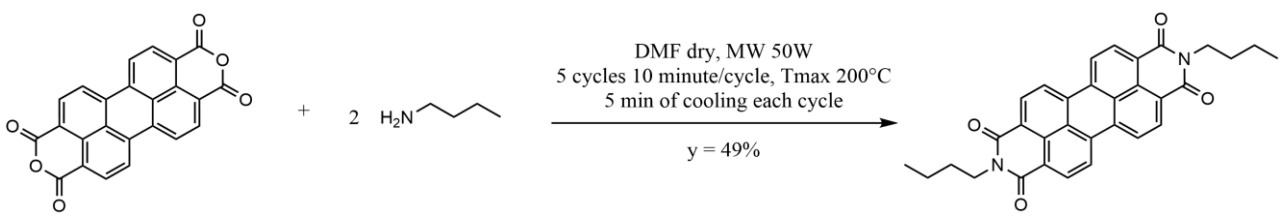

Scheme S1. Synthesis of Per.

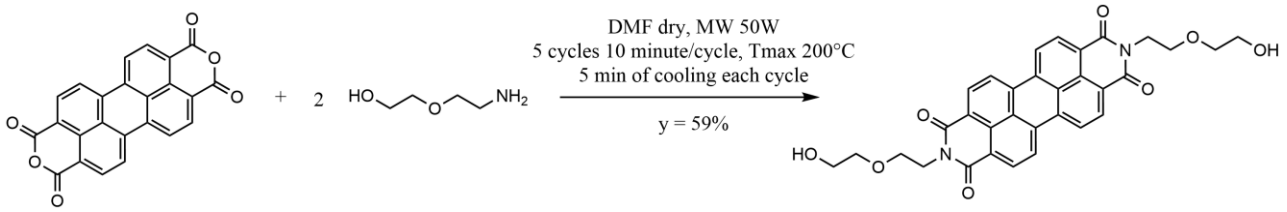

Scheme S2. Synthesis of Per-OH.

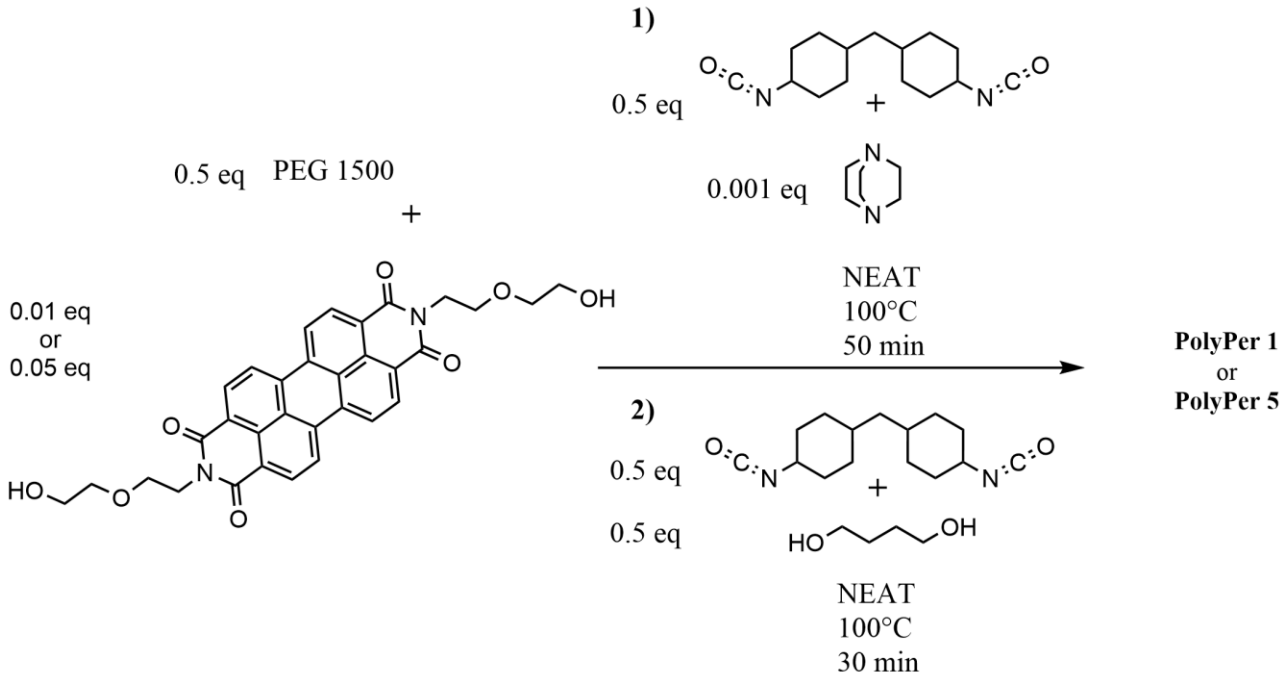

Scheme S3. Synthesis of PolyPer1 and PolyPer5.

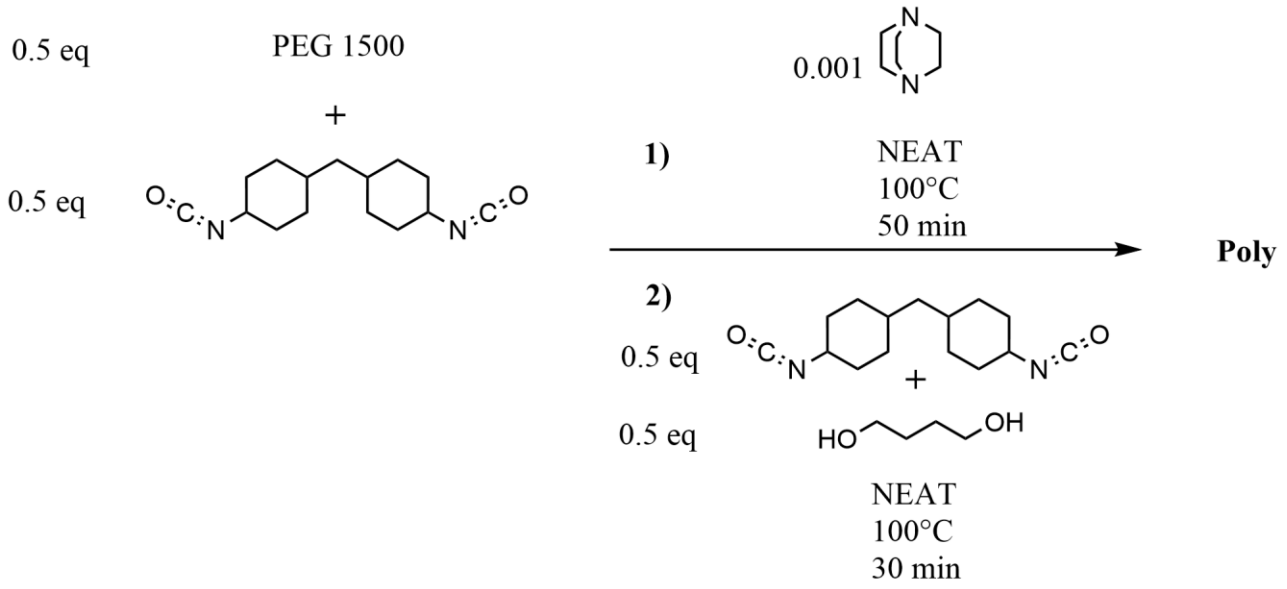

Scheme S4. Synthesis of Poly.

2. NMR

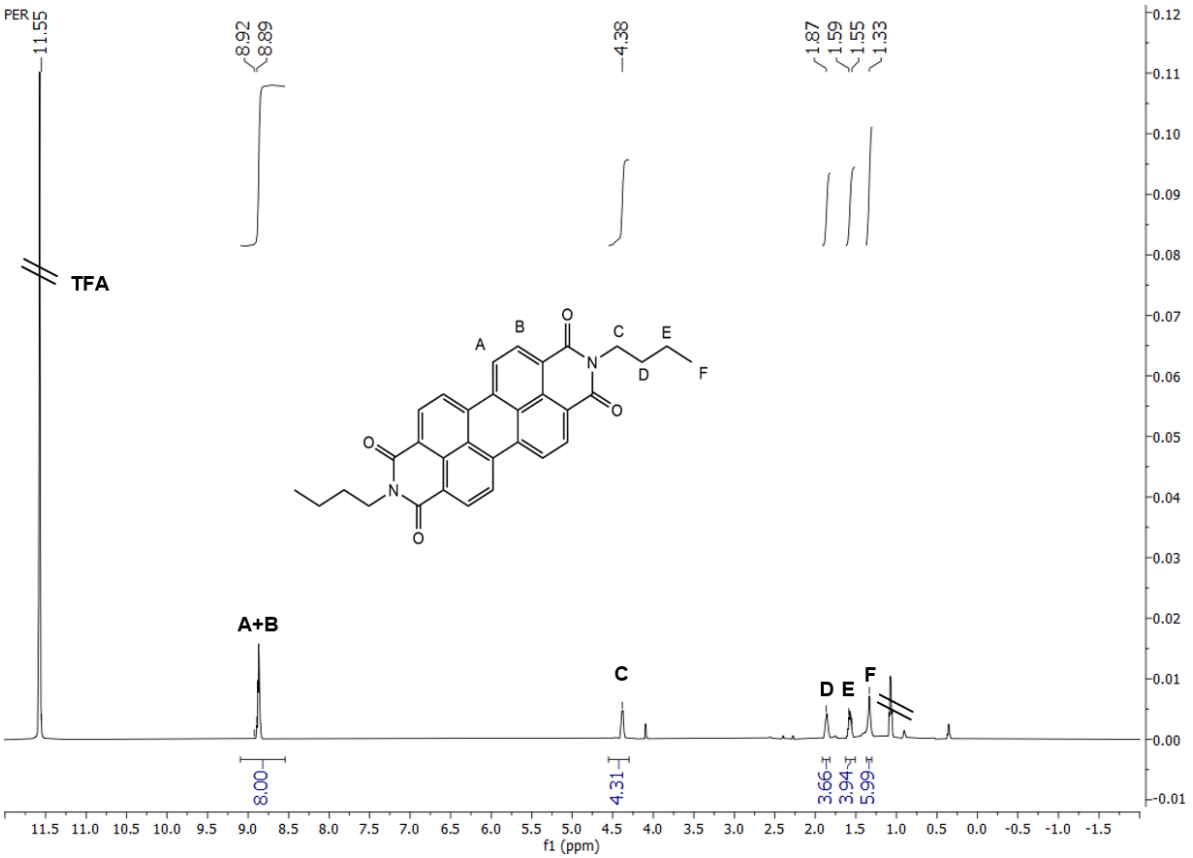

Figure S1. ^{1}H NMR of Per (deuterated TFA, 600 MHz, 298 K).

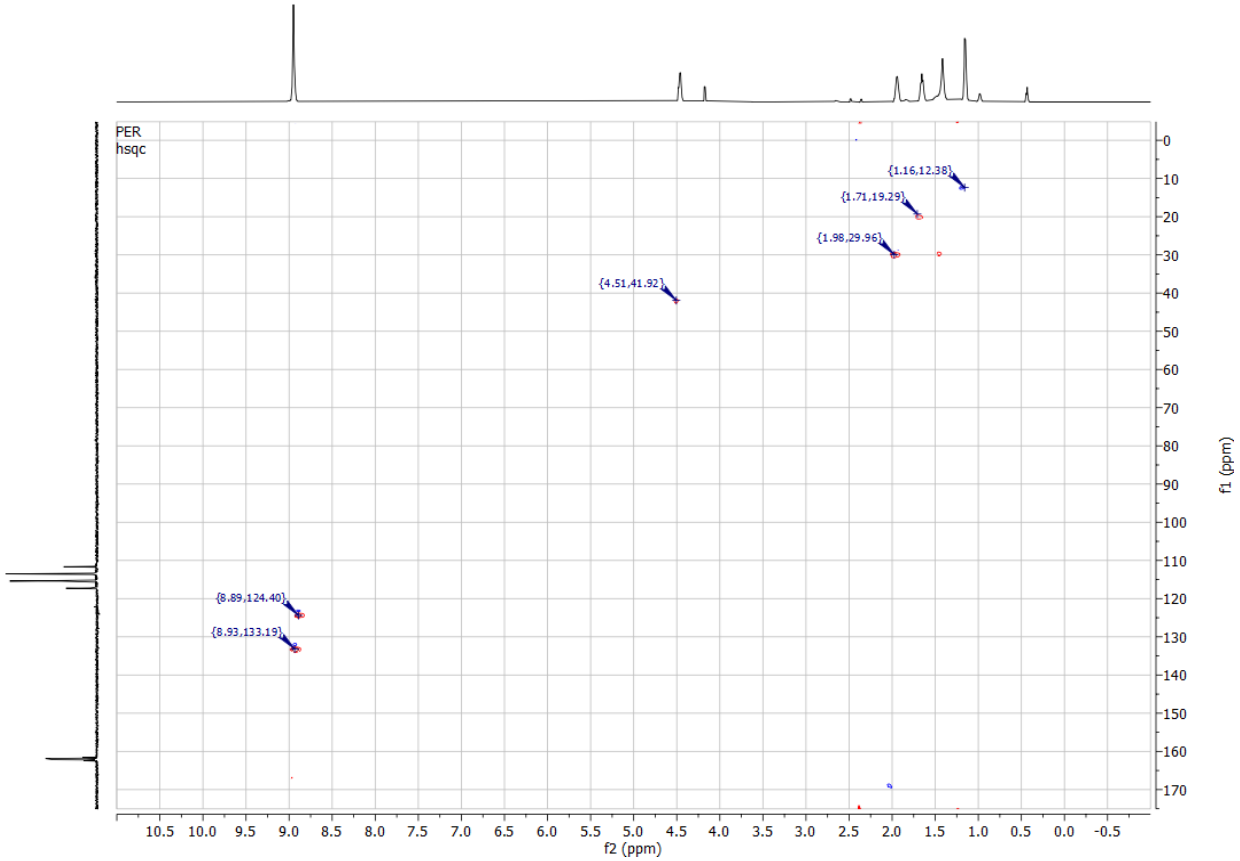

Figure S2. HSQC of Per (deuterated TFA, 151 MHz, 298 K).

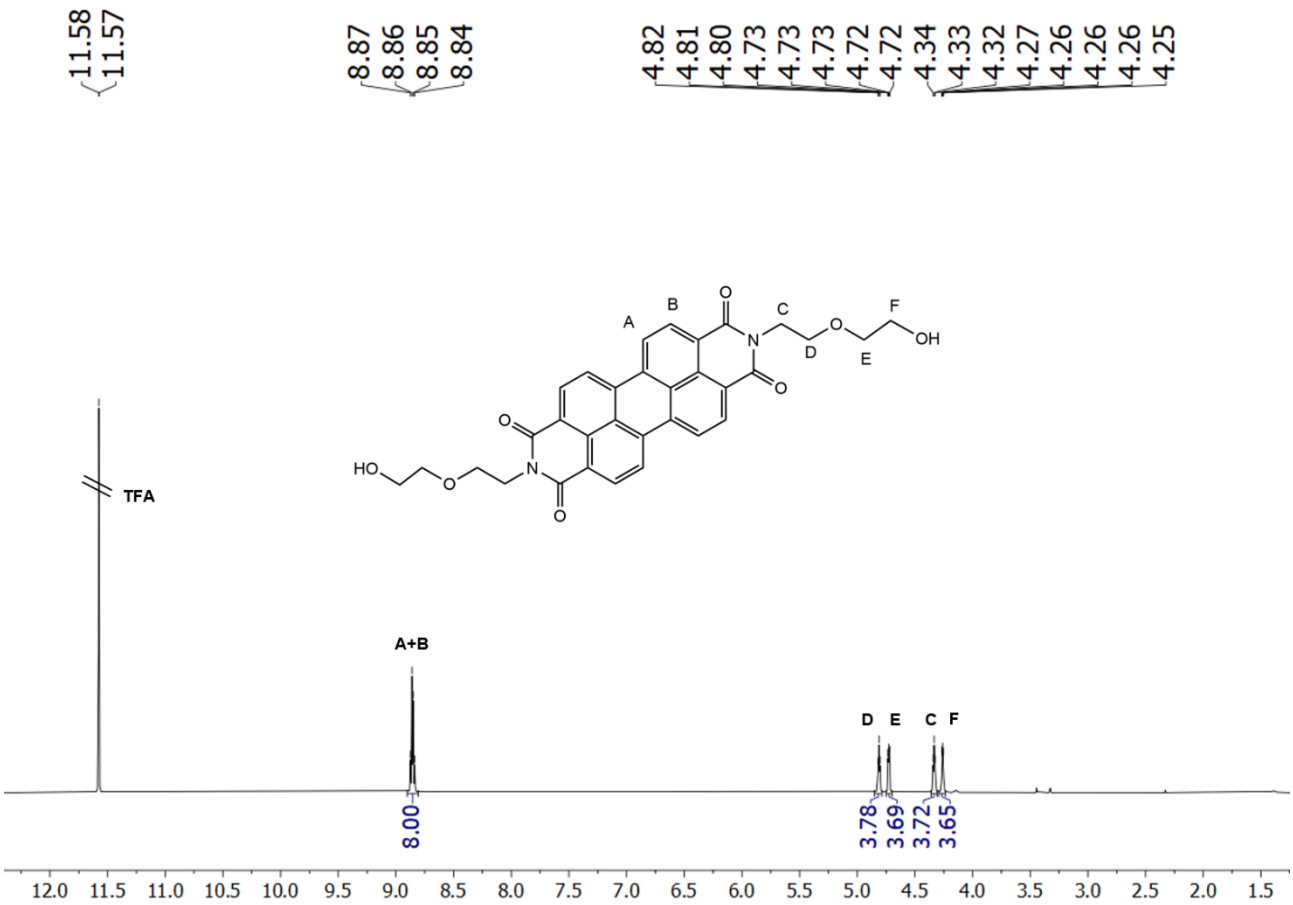

Figure S3. ^{1}H NMR of Per-OH (deuterated TFA, 600 MHz, 298 K).

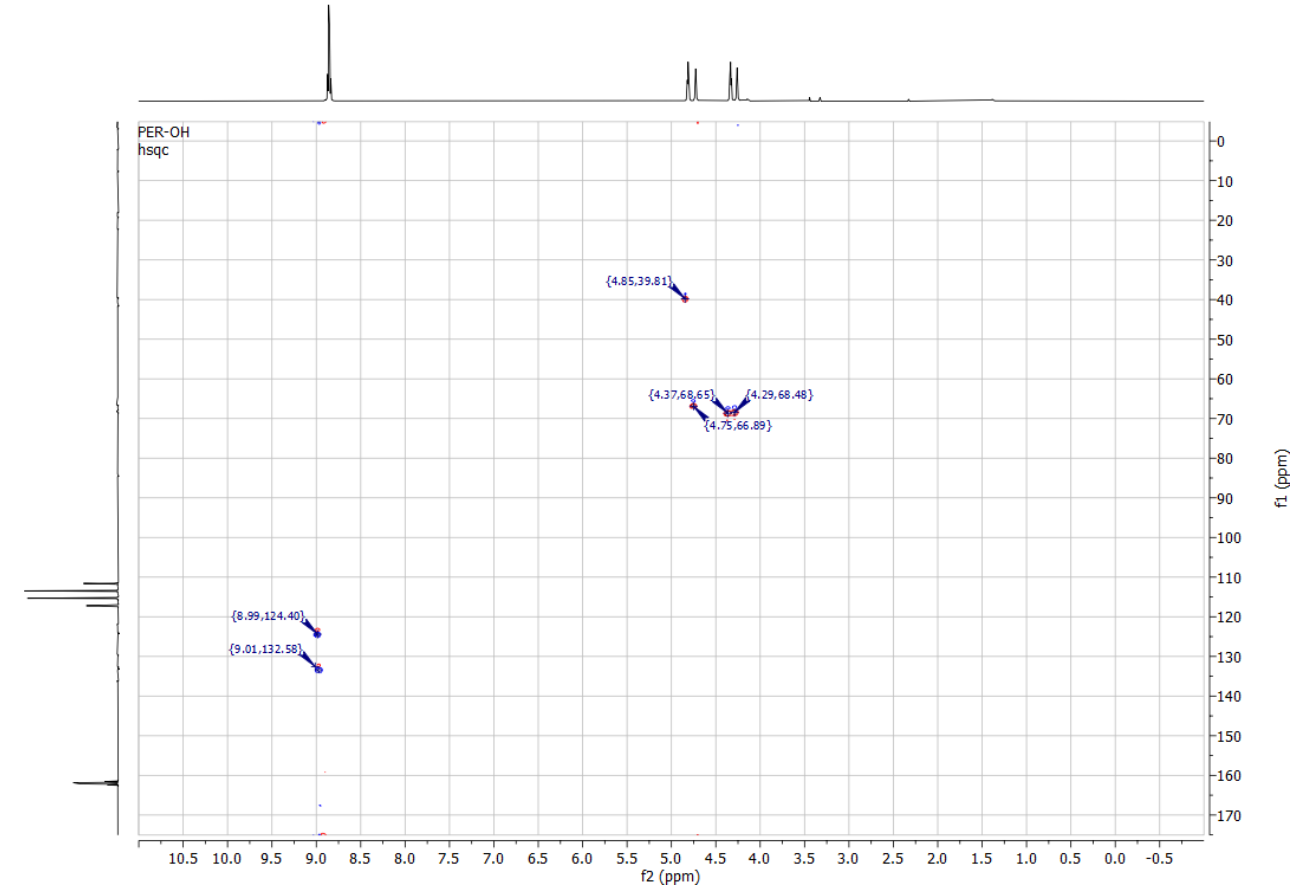

Figure S4. HSQC of Per-OH (deuterated TFA, 151 MHz, 298 K).

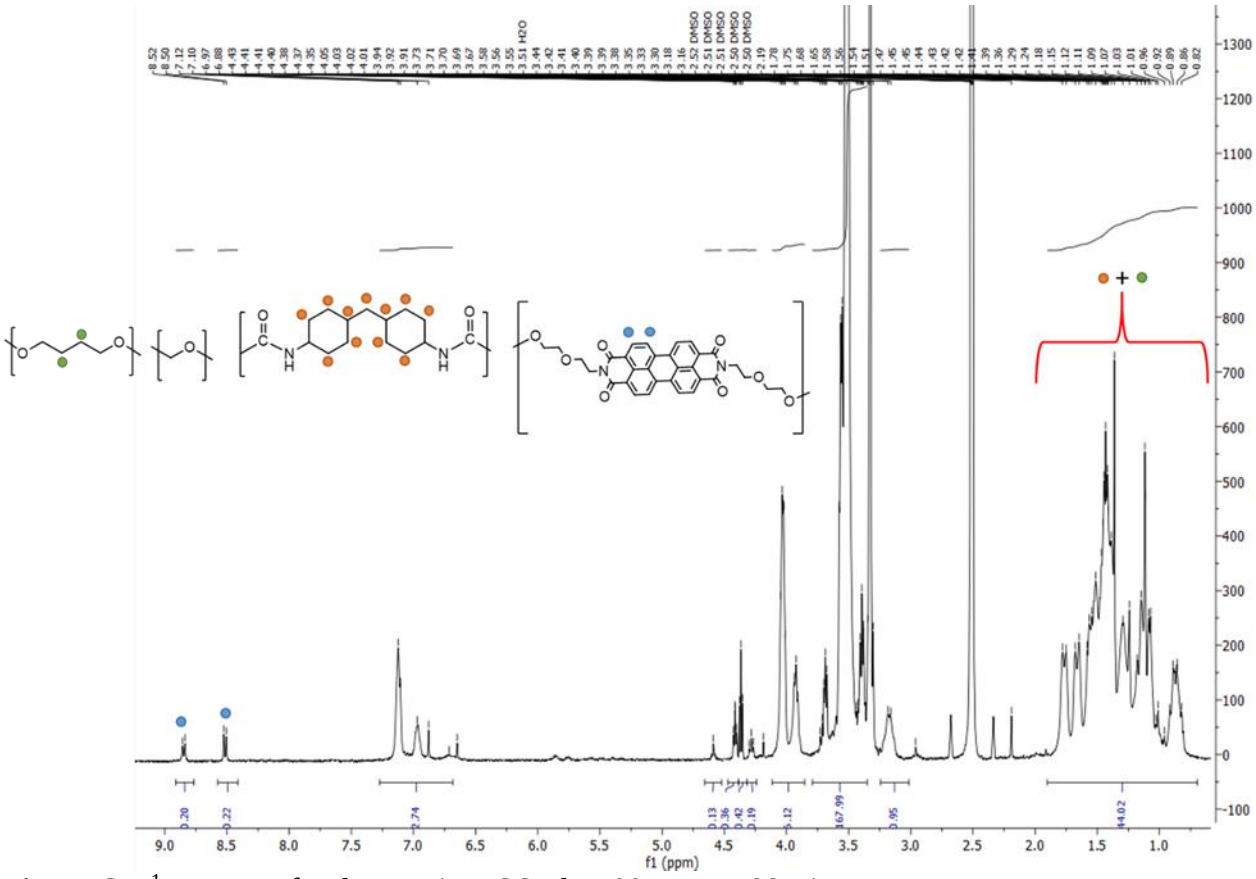

Figure S5. ^{1}H NMR of PolyPer5 (DMSO_d$_6$, 400 MHz, 298 K).

3. Gel Permeation Chromatography

Table S1. GPC data of TPU, Poly, PolyPer1 and PolyPer5: number average molecular weight (M_n), weight average molecular weight (M_w) and polydispersity index (Đ).

Sample	**M_n [g mol^{-1}]**	**M_w [g mol^{-1}]**	**Đ**
TPU	93410	310570	3.3
PEG1500	660	870	1.3
Poly	1960	3630	1.9
PolyPer1	1960	3360	1.7
PolyPer5	2300	4640	2.0

4. Calorimetric data of bulk PU and Films

Table S2. Calorimetric data of bulk PU and films.

Sample	T_g [°C]	ΔC_p [J·g^{-1}·°C^{-1}]	T_m [°C]	ΔH_m (PEG segments) [J·g^{-1}]
Poly[a]	-45	0.16	42	63.1
PolyPer1[a]	-46	0.18	36	52.6
PolyPer5[a]	-46	0.11	32	40.1
D-0.15[b]	-45	0.37	44	12.2
D-0.78[b]	-46	0.23	41	15.6
MC-0.15[b]	-44	0.36	40	11.8
MC-0.78[b]	-43	0.39	42	8.3

a) Calorimetric data are referred to the heating scan after controlled cooling at 10 °C min^{-1}.

b) Calorimetric data are referred to the first heating scan.

5. DSC and calorimetric data of TPU

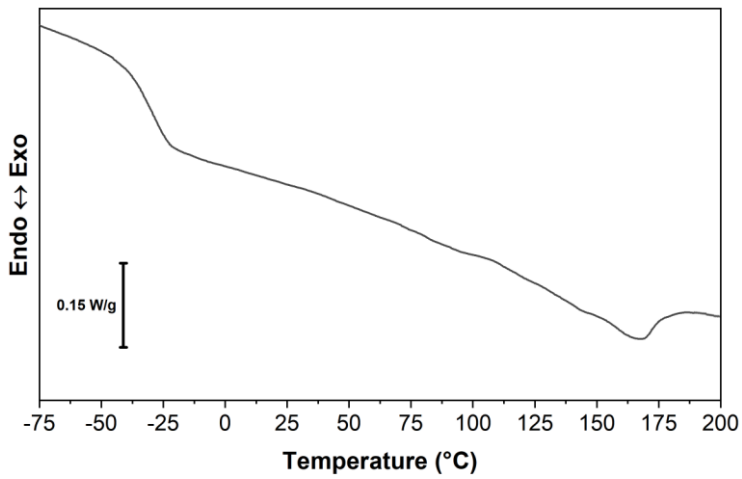

Figure S6. DSC scans after controlled cooling at 10 °C min^{-1} of TPU.

Table S3. Calorimetric data are referred to the heating scan after controlled cooling at 10 °C min^{-1}.

Sample	T_g [°C]	ΔC_p [$J \cdot g^{-1} \cdot °C^{-1}$]	T_m [°C]	ΔH_m [$J \cdot g^{-1}$]
TPU	-30	0.41	164	13.4

6. DMTA analysis

DMTA analysis was carried out to shed light on the miscibility between **Poly** and **TPU**. The pristine materials display a single loss modulus peak (as well as a single tanδ peak) ascribable to the glass transition, located at -52 °C for **Poly** and at -32 °C for **TPU**. Likewise, the analyzed blend (**MC-0.15**) shows a single peak of loss modulus at the intermediate temperature of -45°C. Therefore, in the blend, the TPU and the synthetized PU form a single miscible amorphous phase.

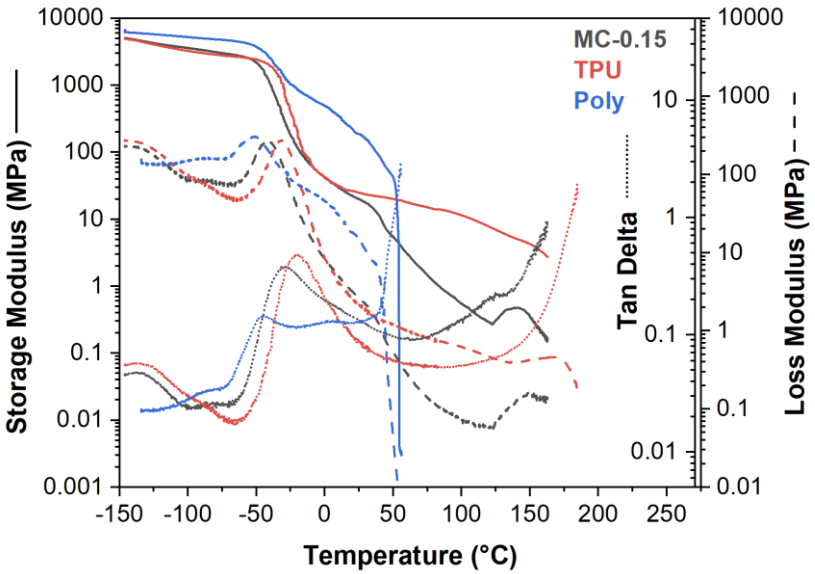

Figure S7. DMTA analysis of **MC-0.15** (black), **TPU** (red), and **Poly** (blue). Storage modulus (solid line), loss modulus (dashed line) and tanδ (dotted line) are reported.

7. Mechanical data and pictures under UV light of D and MC samples

Table S4. Mechanical data of **D** and **MC** samples.

Sample	Stress at break [MPa]	Strain at break [%]	Young's Modulus [MPa]
D-0.15	20 ± 3	$1.32 \cdot 10^3 \pm 0.05 \cdot 10^3$	5.3 ± 0,4
D-0.78	17 ± 4	$1.2 \cdot 10^3 \pm 0.1 \cdot 10^3$	6.0 ± 0,3
MC-0.15	19 ± 4	$1.2 \cdot 10^3 \pm 0.1 \cdot 10^3$	5.4 ± 0.4
MC-0.78	18 ± 6	$1.2 \cdot 10^3 \pm 0.1 \cdot 10^3$	6 ± 1

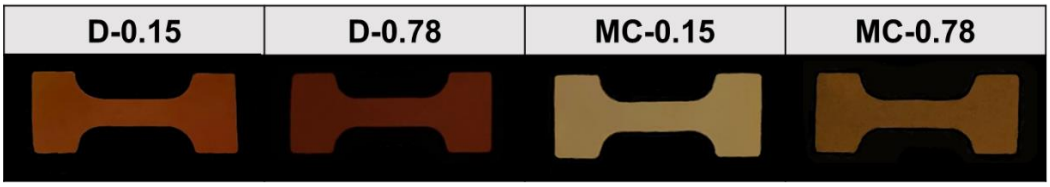

Figure S8. Images under UV light (λ_{ex}=365 nm) of films of **D** and **MC** samples.

8. Mechanochromic characterization

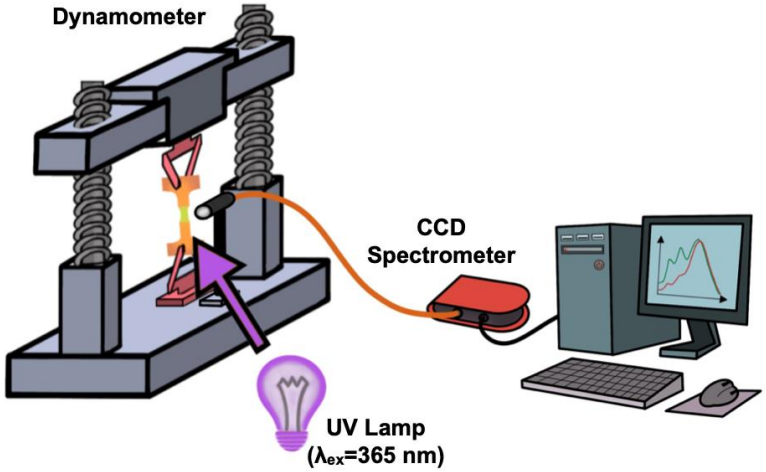

Figure S9. Schematic representation of the setup employed for the mechanochromic characterizations.

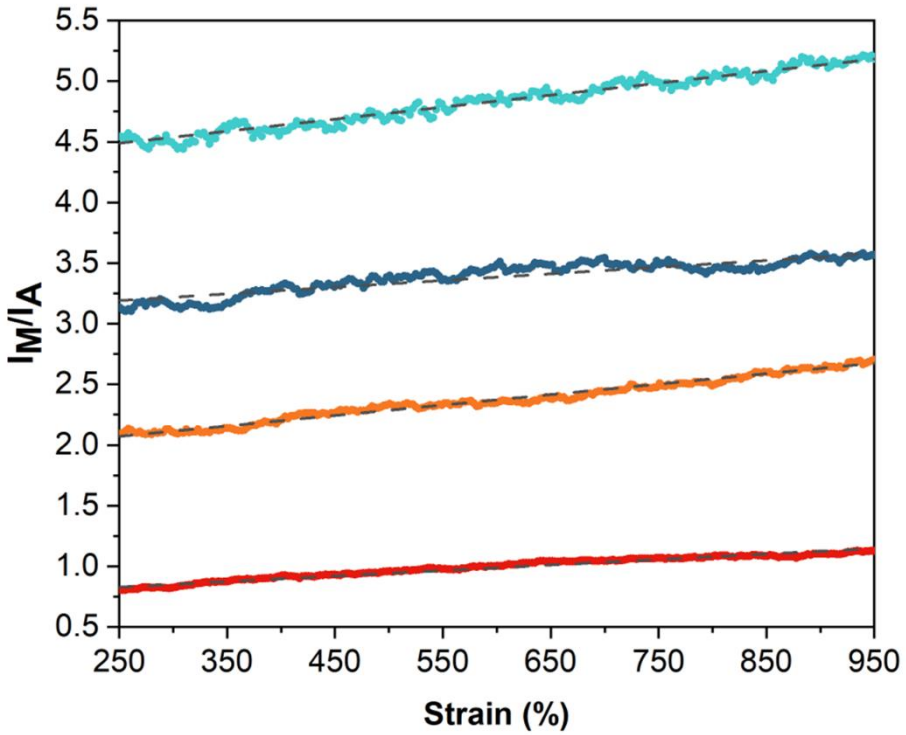

Figure S10. I_M/I_A (dots) plotted versus strain in the range 250% - 950%, fitted with a linear function (dashed line): D-0.15 (orange), D-0.78 (red), MC-0.15 (cyan,) and MC 0.78 (blue). The results reported are averaged among three samples.

Table S5. Results of the linear fit for D and MC samples.

Sample	Slope	R^2
D-0.15	$8.62 \cdot 10^{-4} \pm 0.07 \cdot 10^{-4}$	0.98
D-0.78	$4.55 \cdot 10^{-4} \pm 0.05 \cdot 10^{-4}$	0.97
MC-0.15	$9.9 \cdot 10^{-4} \pm 0.1 \cdot 10^{-4}$	0.96
MC-0.78	$5.5 \cdot 10^{-4} \pm 0.1 \cdot 10^{-4}$	0.86

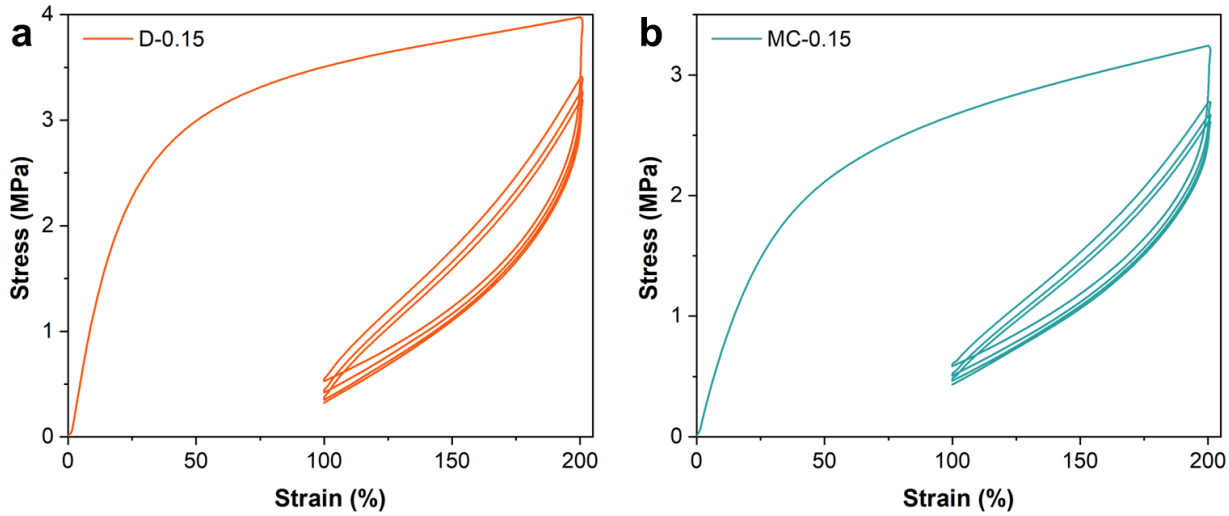

Figure S11. Stress-strain behavior of a) D-0.15 and b) MC-0.15 when deformed through multiple cycles. These stress-strain curves correspond to the loading-unloading cycles reported in Figure 6e and f as a function of time.

Table S6. Calorimetric and mechanochromic data before and after stress-relaxation experiments.

Sample	**Initial ΔH_m [J g^{-1}]**	**ΔH_m after relaxation [J g^{-1}]**	**Initial I_M/I_A**	**I_M/I_A max**	**I_M/I_A after relaxation**
D-0.15	12.2	16.0	1.216	1.44[a]	1.250
D-0.78	15.6	15.9	0.370	0.46[b]	0.336
MC-0.15	11.8	12.4	3.538	4.41[c]	3.294

a) at 135 s

b) at 130 s

c) at 130 s